Analysis Procedures for Evaluating Superheavy Load Movement on Flexible Pavements, Volume X: Appendix I, Analysis Package for Superheavy Load Vehicle Movement on Flexible Pavement (SuperPACK)

PUBLICATION NO. FHWA-HRT-18-058

MARCH 2019

U.S. Department of Transportation
Federal Highway Administration

Research, Development, and Technology
Turner-Fairbank Highway Research Center
6300 Georgetown Pike
McLean, VA 22101-2296

FOREWORD

The movement of superheavy loads (SHLs) on the Nation's highways is an increasingly common, vital economic necessity for many important industries, such as chemical, oil, electrical, and defense. Many superheavy components are extremely large and heavy (gross vehicle weights in excess of a few million pounds), and they often require specialized trailers and hauling units. At times, SHL vehicles have been assembled to suit the load being transported, and therefore, the axle configurations have not been standard or consistent. Accommodating SHL movements without undue damage to highway infrastructure requires the determination of whether the pavement is structurally adequate to sustain the SHL movement and protect any underground utilities. Such determination involves analyzing the likelihood of instantaneous or rapid load-induced shear failure of the pavement structure.

The goal of this project was to develop a comprehensive analysis process for evaluating SHL movement on flexible pavements. As part of this project, a comprehensive mechanistic-based analysis approach consisting of several analysis procedures was developed for flexible pavement structures and documented in a 10-volume series of Federal Highway Administration reports—a final report and 9 appendices.[1–9] This is *Analysis Procedures for Evaluating Superheavy Load Movement on Flexible Pavements, Volume X: Appendix I, Analysis Package for Superheavy Load Vehicle Movement on Flexible Pavement (SuperPACK)*, which describes the analysis software package, SuperPACK, developed for the evaluation of specific cases of SHL movements on flexible pavements. This report is intended for use by highway agency pavement engineers responsible for assessing the structural adequacy of pavements in proposed routes and identifying mitigation strategies, when warranted, in support of transportation agencies' responses to SHL-movement permit requests.

Cheryl Allen Richter, Ph.D., P.E.
Director, Office of Infrastructure
Research and Development

TECHNICAL REPORT DOCUMENTATION PAGE

1. Report No. FHWA-HRT-18-058	2. Government Accession No.	3. Recipient's Catalog No.
4. Title and Subtitle Analysis Procedures for Evaluating Superheavy Load Movement on Flexible Pavements, Volume X: Appendix I, Analysis Package for Superheavy Load Vehicle Movement on Flexible Pavement (SuperPACK)		5. Report Date March 2019 6. Performing Organization Code
7. Author(s) Seyed-Farzan Kazemi (ORCID: 0000-0003-2313-4995), Hadi Nabizadeh (ORCID: 0000-0001-8215-1299), Mohammed Nimeri (ORCID: 0000-0002-3328-4367), Dario Batioja-Alvarez (ORCID: 0000-0002-1094-553X), Elie Y. Hajj (ORCID: 0000-0001-8568-6360), Raj V. Siddharthan (ORCID: 0000-0002-3847-7934), and Adam J.T. Hand (ORCID: 0000-0002-5041-7491)		8. Performing Organization Report No. WRSC-UNR-201710-01I
9. Performing Organization Name and Address Department of Civil and Environmental Engineering University of Nevada Reno, NV 89557		10. Work Unit No. 11. Contract or Grant No. DTFH61-13-C-00014
12. Sponsoring Agency Name and Address Office of Infrastructure Research and Development Federal Highway Administration 6300 Georgetown Pike McLean, VA 22101		13. Type of Report and Period Covered Final Report; August 2013–July 2018 14. Sponsoring Agency Code HRDI-20
15. Supplementary Notes Nadarajah Sivaneswaran (HRDI-20; ORCID: 0000-0003-0287-664X), Office of Infrastructure Research and Development, Turner-Fairbank Highway Research Center, served as the Contracting Officer's Representative.		

16. Abstract

The movement of superheavy loads (SHLs) has become more common over the years, since it is a vital necessity for many important industries, such as chemical, oil, electrical, and defense. SHL hauling units are much larger in size and weight compared to standard trucks. SHL vehicles' gross vehicle weights may be in excess of a few million pounds, so they often require specialized trailers and components with nonstandard spacing between tires and axles. Accommodating SHL movements requires the determination of whether the pavement is structurally adequate and involves the analysis of the likelihood of instantaneous or rapid load-induced shear failure.

As part of this Federal Highway Administration project, Analysis Procedures for Evaluating Superheavy Load Movement on Flexible Pavements, an analysis package, Superheavy Load Vehicle Movement on Flexible Pavement (SuperPACK), was developed to evaluate specific cases of SHL-vehicle movements. This report describes the major components of SuperPACK: preanalysis modules (A modules), analysis modules (B modules), and an analysis engine (3D-Move ENHANCED).[10] The A modules, which are required to proceed to the B modules, require information on vehicle axle configurations, material properties, subgrade shear strength parameters, and representative material properties for the analysis and reference vehicles. The B modules conduct bearing capacity, service limit, slope stability, buried utility, and cost allocation analyses. All the A and B modules require pavement responses, excepting the module on vehicle axle configurations. 3D-Move ENHANCED was developed to provide the modules with responses based upon the request.[10]

17. Key Words	18. Distribution Statement
Superheavy load, 3D-Move ENHANCED, pavement response, bearing capacity, buried utility, cost allocation	No restrictions. This document is available to the public through the National Technical Information Service, Springfield, VA 22161. http://www.ntis.gov

19. Security Classif. (of this report)	20. Security Classif. (of this page)	21. No. of Pages	22. Price
Unclassified	Unclassified	47	N/A

SI* (MODERN METRIC) CONVERSION FACTORS

APPROXIMATE CONVERSIONS TO SI UNITS

Symbol	When You Know	Multiply By	To Find	Symbol
		LENGTH		
in	inches	25.4	millimeters	mm
ft	feet	0.305	meters	m
yd	yards	0.914	meters	m
mi	miles	1.61	kilometers	km
		AREA		
in^2	square inches	645.2	square millimeters	mm^2
ft^2	square feet	0.093	square meters	m^2
yd^2	square yard	0.836	square meters	m^2
ac	acres	0.405	hectares	ha
mi^2	square miles	2.59	square kilometers	km^2
		VOLUME		
fl oz	fluid ounces	29.57	milliliters	mL
gal	gallons	3.785	liters	L
ft^3	cubic feet	0.028	cubic meters	m^3
yd^3	cubic yards	0.765	cubic meters	m^3
		NOTE: volumes greater than 1000 L shall be shown in m^3		
		MASS		
oz	ounces	28.35	grams	g
lb	pounds	0.454	kilograms	kg
T	short tons (2000 lb)	0.907	megagrams (or "metric ton")	Mg (or "t")
		TEMPERATURE (exact degrees)		
^oF	Fahrenheit	5 (F-32)/9 or (F-32)/1.8	Celsius	^oC
		ILLUMINATION		
fc	foot-candles	10.76	lux	lx
fl	foot-Lamberts	3.426	$candela/m^2$	cd/m^2
		FORCE and PRESSURE or STRESS		
lbf	poundforce	4.45	newtons	N
lbf/in^2	poundforce per square inch	6.89	kilopascals	kPa

APPROXIMATE CONVERSIONS FROM SI UNITS

Symbol	When You Know	Multiply By	To Find	Symbol
		LENGTH		
mm	millimeters	0.039	inches	in
m	meters	3.28	feet	ft
m	meters	1.09	yards	yd
km	kilometers	0.621	miles	mi
		AREA		
mm^2	square millimeters	0.0016	square inches	in^2
m^2	square meters	10.764	square feet	ft^2
m^2	square meters	1.195	square yards	yd^2
ha	hectares	2.47	acres	ac
km^2	square kilometers	0.386	square miles	mi^2
		VOLUME		
mL	milliliters	0.034	fluid ounces	fl oz
L	liters	0.264	gallons	gal
m^3	cubic meters	35.314	cubic feet	ft^3
m^3	cubic meters	1.307	cubic yards	yd^3
		MASS		
g	grams	0.035	ounces	oz
kg	kilograms	2.202	pounds	lb
Mg (or "t")	megagrams (or "metric ton")	1.103	short tons (2000 lb)	T
		TEMPERATURE (exact degrees)		
^oC	Celsius	1.8C+32	Fahrenheit	^oF
		ILLUMINATION		
lx	lux	0.0929	foot-candles	fc
cd/m^2	$candela/m^2$	0.2919	foot-Lamberts	fl
		FORCE and PRESSURE or STRESS		
N	newtons	0.225	poundforce	lbf
kPa	kilopascals	0.145	poundforce per square inch	lbf/in^2

*SI is the symbol for the International System of Units. Appropriate rounding should be made to comply with Section 4 of ASTM E380.
(Revised March 2003)

ANALYSIS PROCEDURES FOR EVALUATING SUPERHEAVY LOAD MOVEMENT ON FLEXIBLE PAVEMENTS PROJECT REPORT SERIES

This volume is the 10th of 10 volumes in this research report series. Volume I is the final report, and Volume II through Volume X consist of Appendix A through Appendix I. Any reference to a volume in this series will be referenced in the text as "Volume II: Appendix A," "Volume III: Appendix B," and so forth. The following list contains the volumes:

Volume	Title	Report Number
I	Analysis Procedures for Evaluating Superheavy Load Movement on Flexible Pavements, Volume I: Final Report	FHWA-HRT-18-049
II	Analysis Procedures for Evaluating Superheavy Load Movement on Flexible Pavements, Volume II: Appendix A, Experimental Program	FHWA-HRT-18-050
III	Analysis Procedures for Evaluating Superheavy Load Movement on Flexible Pavements, Volume III: Appendix B, Superheavy Load Configurations and Nucleus of Analysis Vehicle	FHWA-HRT-18-051
IV	Analysis Procedures for Evaluating Superheavy Load Movement on Flexible Pavements, Volume IV: Appendix C, Material Characterization for Superheavy Load Movement Analysis	FHWA-HRT-18-052
V	Analysis Procedures for Evaluating Superheavy Load Movement on Flexible Pavements, Volume V: Appendix D, Estimation of Subgrade Shear Strength Parameters Using Falling Weight Deflectometer	FHWA-HRT-18-053
VI	Analysis Procedures for Evaluating Superheavy Load Movement on Flexible Pavements, Volume VI: Appendix E, Ultimate and Service Limit Analyses	FHWA-HRT-18-054
VII	Analysis Procedures for Evaluating Superheavy Load Movement on Flexible Pavements, Volume VII: Appendix F, Failure Analysis of Sloped Pavement Shoulders	FHWA-HRT-18-055
VIII	Analysis Procedures for Evaluating Superheavy Load Movement on Flexible Pavements, Volume VIII: Appendix G, Risk Analysis of Buried Utilities Under Superheavy Load Vehicle Movements	FHWA-HRT-18-056
IX	Analysis Procedures for Evaluating Superheavy Load Movement on Flexible Pavements, Volume IX: Appendix H, Analysis of Cost Allocation Associated with Pavement Damage Under a Superheavy Load Vehicle Movement	FHWA-HRT-18-057
X	Analysis Procedures for Evaluating Superheavy Load Movement on Flexible Pavements, Volume X: Appendix I, Analysis Package for Superheavy Load Vehicle Movement on Flexible Pavement (SuperPACK)	FHWA-HRT-18-058

TABLE OF CONTENTS

LIST OF FIGURES

LIST OF TABLES

LIST OF ACRONYMS AND SYMBOLS

Abbreviations

2D	two dimensional
3D	three dimensional
AC	asphalt concrete
FEM	finite element method
FFT	fast Fourier transform
FWD	falling weight deflectometer
GUI	graphical user interface
MATLAB	Matrix Laboratory
ME	mechanistic–empirical
MLET	multilayer linear elastic theory
PDAC	pavement damage–associated costs
SG	subgrade
SHL	superheavy load
SuperPACK	Superheavy Load Pavement Analysis PACKage

Symbols

A_{mn}	Fourier coefficient matrix
A_{1j} to A_{4j}	unknown displacement coefficients for each pavement layer
B_{f1} to B_{f3}, K_{f1} to K_{f3}	asphalt concrete bottom–up fatigue cracking calibration factors
B_{r1} to B_{r3}, K_{r1} to K_{r3}	asphalt concrete permanent deformation calibration factors
c	cohesion
E^*	dynamic modulus
FWD_{equiv}	equivalent falling weight deflectometer load level
G	second Lamé parameter
H	thickness of pavement layer
H_N	location of the bottom boundary with respect to the last layer interface
i	layer number
j	directional index (j = 1 for x-direction, j = 2 for y-direction, and j = 3 for z-direction)
K_{xx}	shear slippage stiffness in x-direction
K_{yy}	shear slippage stiffness in y-direction
M	total number of waves in x-direction
m	wave number in x-direction
M_R	resilient modulus
N	total number of waves in y-direction
N_L	number of layers
N_x	number of additional tires in x-direction
N_y	number of additional tires in y-direction
n	wave number in y-direction
n_1	first eigenvalue for the pavement system
n_2	second eigenvalue for the pavement system

$p(x, y)$	vertical stress for a point with coordinates of (x, y)
q_u	ultimate bearing capacity
t	time
$tr(.)$	field trace function (summation)
u_1	displacement in x-direction
u_2	displacement in y-direction
u_3	displacement in z-direction
$u_1^-(H_i)$	displacement in x-direction at the bottom of layer i
$u_2^-(H_i)$	displacement in y-direction at the bottom of layer i
$u_j(x,y,z,t)$	displacement in j-direction at location of interest
$\tilde{u}_1^+(0)$	displacement in x-direction on top of layer $i + 1$ (frequency domain)
$\tilde{u}_2^+(0)$	displacement in y-direction on top of layer $i + 1$ (frequency domain)
$\tilde{u}_j(z)$	displacement in j-direction at location of interest in the frequency domain
$\tilde{u}_j^-(\omega_x, \omega_y, H)$	displacement in j-direction at the bottom of upper layer (frequency domain)
$\tilde{u}_j^+(\omega_x, \omega_y, 0)$	displacement in j-direction on top of lower layer (frequency domain)
V	superheavy load–vehicle speed
V_a	air void
V_{beff}	effective binder content
$\tilde{\varepsilon}$	strain tensor (frequency domain)
ε_{jj}	normal strain in j-direction (spatial domain)
ε_{jk}	shear strain on the plane with normal in the j-direction and stretching in the k-direction (spatial domain).
ε_{kj}	shear strain on the plane with normal in the k-direction and stretching in the j-direction (spatial domain)
$\tilde{\varepsilon}_{jj}$	normal strain in j-direction (frequency domain)
λ	first Lamé parameter
ρ	material density
σ_{jj}	normal stress in j-direction (spatial domain)
σ_{jk}	shear stress on the plane with normal in the j-direction and stretching in the k-direction (spatial domain)
$\tilde{\sigma}_{jj}$	normal stress in j-direction (frequency domain)
$\tilde{\sigma}_{jz}^-(\omega_x, \omega_y, H)$	stress at the bottom of upper layer (frequency domain)
$\tilde{\sigma}_{jz}^+(\omega_x, \omega_y, 0)$	stress at the top of lower layer (frequency domain)
τ_{max}	maximum shear strength
$\tau_{xz}^i(H_i)$	longitudinal shear stress at the interface of layers i and $i + 1$
$\tau_{yz}^i(H_i)$	lateral shear stress at the interface of layers i and $i + 1$
ϕ	angle of internal friction
ω_x	spatial frequency in x-direction
ω_y	spatial frequency in y-direction
ω_t	angular frequency

CHAPTER 1. INTRODUCTION

Appropriate, timely, and precise evaluation of the consequences of a specific superheavy load (SHL) movement is essential for highway agencies, particularly when a variety of scenarios should be considered. Needed analyses and their interactions are presented in a flowchart of the overall approach developed as part of this project (figure 1). As shown in figure 1, the first step of the approach involves a risk analysis of instantaneous or rapid load-induced ultimate shear failure. As the subgrade (SG) is generally the weakest layer in a pavement structure, bearing failure analysis investigates the likelihood of general bearing capacity failure under an SHL vehicle within the influenced zone of an SG layer. Next, the sloped-shoulder failure analysis examines the bearing capacity failure and edge slope stability associated with the sloping ground under an SHL-vehicle movement. Once the ultimate failure analyses are investigated and ruled out, when applicable, a buried utility risk analysis is conducted. In this analysis, the induced stresses and deflections by an SHL vehicle on existing buried utilities are evaluated and compared to established design criteria. Subsequently, if no mitigation strategies are needed, service limit analyses for localized shear failure and a deflection-based service limit are conducted. The localized shear failure analysis investigates the possibility of failure at the critical location on top of the SG layer under an SHL vehicle. The deflection-based service limit analysis assesses the magnitude of the load-induced pavement deflections during an SHL movement. For instance, this analysis may suggest the need for mitigation strategies to meet the imposed acceptable surface deflection limits. After successfully completing all previously described analyses (i.e., ultimate failure analyses, buried utility risk analysis, and service limit analyses), a cost allocation analysis is conducted. This analysis allows for the estimation of pavement damage–associated costs (PDAC) resulting from an SHL movement on a flexible pavement.

1.1. OBJECTIVES AND SCOPE OF WORK

As part of this Federal Highway Administration project, Analysis Procedures for Evaluating Superheavy Load Movement on Flexible Pavements, a comprehensive mechanistic-based analysis approach consisting of several analysis procedures was developed. Table 1 is a summary of the various analysis procedures that have been developed and the associated objectives (including related volume numbers). This report (Volume X: Appendix I) is the 10th of 10 volumes and describes the comprehensive, user-friendly analysis software package, Superheavy Load Pavement Analysis PACKage (SuperPACK), that was developed for the evaluation of specific cases of SHL movements on flexible pavements.[1–9]

Calculations associated with the analyses presented in figure 1 and table 1 are complex, require pavement responses, and sometimes involve an iterative process. Accordingly, SuperPACK was developed and comprises three main components: preanalysis modules (A modules), analysis modules (B modules), and an analysis engine. These components are briefly explained in this chapter and discussed in more detail in the following chapters.

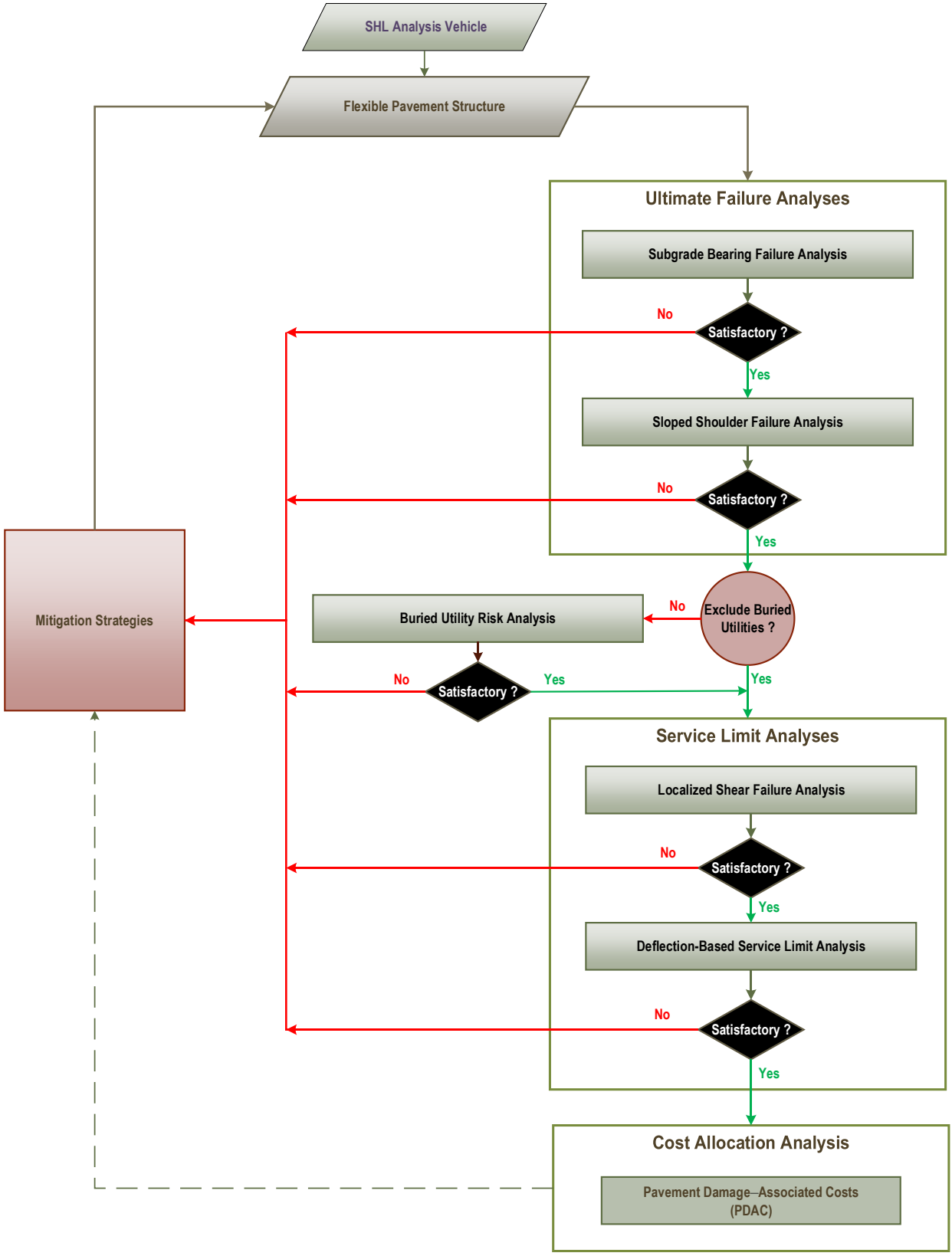

Figure 1. Flowchart. Overall SHL-vehicle analysis methodology.

Table 1. Developed analysis procedures to evaluate SHL movement on flexible pavements.

Procedure	Objective
SHL analysis vehicle	Identify segment(s) of the SHL-vehicle configuration that can be regarded as representative of the entire SHL vehicle (Volume III: Appendix B)[3]
Flexible pavement structure	Characterize representative material properties for existing pavement layers (Volume IV: Appendix C and Volume V: Appendix D)[4,5]
SG bearing failure analysis	Investigate instantaneous ultimate shear failure in pavement SG (Volume VI: Appendix E)[6]
Sloped-shoulder failure analysis	Examine the stability of sloped pavement shoulders under SHL-vehicle movement (Volume VII: Appendix F)[7]
Buried utility risk analysis	Perform risk analysis of existing buried utilities (Volume VIII: Appendix G)[8]
Localized shear failure analysis	Inspect the likelihood of localized failure (yield) in the pavement SG (Volume VI: Appendix E)[6]
Deflection-based service limit analysis	Investigate the development of premature surface distresses (Volume VI: Appendix E)[6]
Cost allocation analysis	Determine pavement damage–associated cost attributable to SHL-vehicle movement (Volume IX: Appendix H)[9]

Figure 2 illustrates the SuperPACK main window. In this figure, the pavement structure, nondestructive testing, preanalysis, and analysis sections are presented. In the pavement structure section, the user fills in the initial information needed for 3D-Move ENHANCED analysis. The A modules use this information as well as certain pavement responses to obtain inputs, which are needed later for the B modules. Figure 2 and other screenshots show important windows of the current version. The structure of these windows is expected to remain similar even after modifications based on feedback from reviewers and users are made.

In this chapter, the A and then B modules are discussed. The A modules must be completed to proceed to the B modules. Since pavement responses may be needed for the A modules, relevant inputs for 3D-Move ENHANCED must be entered by the SuperPACK user before advancing to this set of modules.[10] These parameters may include, but are not limited to, pavement structure, pavement temperature, material type (i.e., liner elastic, stress-dependent, viscoelastic), material density, Poisson's ratio, falling weight deflectometer (FWD) test data (if available), and groundwater table depth. The final section in this chapter is dedicated to the 3D-Move ENHANCED analysis engine with a description of how it interacts with other SuperPACK components.

While this chapter attempts to provide a general overview for the A modules, B modules, and analysis engine, the following chapters provide detailed information for these three analysis-related components. Chapter 2 describes the formulation of 3D-Move ENHANCED, and chapter 3 provides the details of the A and B modules in terms of inputs, outputs, and information needed to undertake the calculation steps presented in the other volumes.[1–9]

Finally, chapter 4 presents the summary, conclusions, and recommendations for future improvements to SuperPACK.

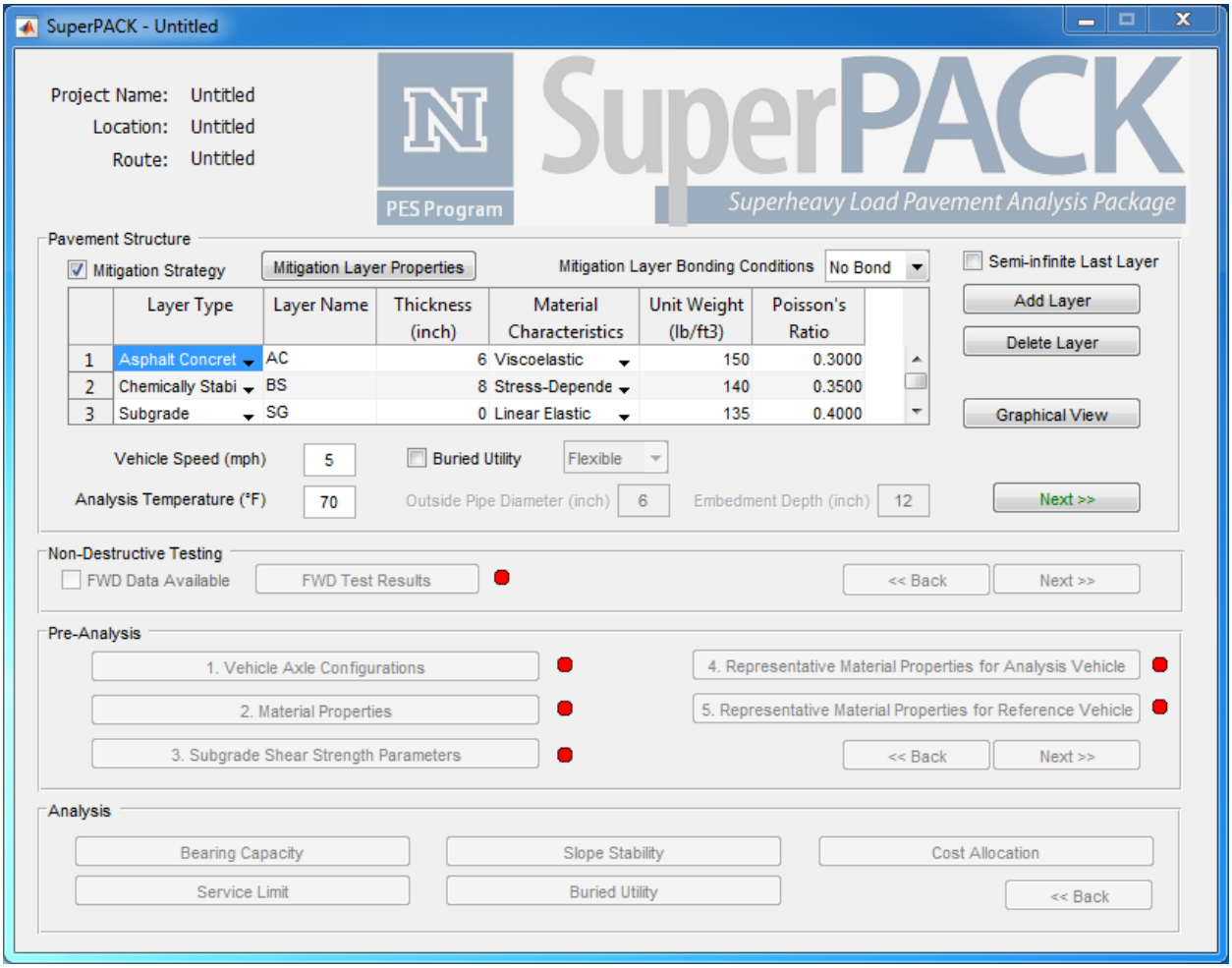

Figure 2. Screenshot. SuperPACK main window.

1.2. PREANALYSIS MODULE COMPONENT

As presented in figure 2, the five A modules investigate the following:

- Vehicle axle configurations (module A1).
- Material properties (module A2).
- SG maximum shear strength (τ_{max}) parameters (module A3).
- Representative material properties for analysis vehicle (module A4).
- Representative material properties for reference vehicle (module A5).

Each of these modules requires specific inputs and outputs. Although these modules may present sets of outputs to a user, these outputs are primarily used in the B modules. If pavement responses are required for a specific A module, that module needs to establish a connection to

3D-Move ENHANCED and inquire the pavement responses of interest. All the A modules need to be connected to 3D-Move ENHANCED, with the exception of module A1.[10]

There is a graphical user interface (GUI) associated with every A module (module GUI). For a particular A module, there are different categories for input and output parameters. Inputs are either entered in the main GUI before running the A module or obtained from the respective module GUI. A modules conduct internal computations to provide the user with desired outputs. For example, cohesion (c) and angle of internal friction (ϕ) are the outputs of module A3. Module outputs are transferred to the main window. In module A3, input parameters for calculating c and ϕ are collected from three sources: inputs, such as pavement structure and material types, provided by the user in the main window; inputs provided by the user in the module A3 GUI; and inputs obtained from 3D-Move ENHANCED (pavement responses). After completing the A modules, the user will be able to proceed to the B modules.

1.3. ANALYSIS MODULE COMPONENT

As presented in figure 2, the five B modules investigate the following:

- Bearing capacity (module B1).
- Service limit (module B2).
- Slope stability (module B3).
- Buried utility (module B4).
- Cost allocation (module B5).

Each of these modules provides users with comprehensive information on the analysis of interest. This key information is valuable to highway agencies when deciding whether an SHL vehicle should be allowed on a road section. Based on the key information, additional analyses, such as mitigation strategies, might need to be investigated according to the flowchart presented in figure 1.

All five B modules use the information provided by the user as well as specific information from the main GUI and 3D-Move ENHANCED in their respective module GUIs. Typically, each of the B modules includes certain criteria to determine if a pavement structure can accommodate a given SHL-vehicle movement without jeopardizing pavement performance or serviceability. However, there are no criteria for cost allocation due to the damage induced by an SHL-vehicle movement. For module B5, the highway agency needs to apply engineering judgment to evaluate if PDAC are reasonable and could be compensated for by collecting permit fees. Each of the other four B modules (i.e., B1 through B4) contains built-in pass–fail criteria, and when any one of the criteria is not met, the responsible highway agency has three options: avoid the SHL-vehicle movement, take an alternative action, or explore a mitigation strategy to improve the pavement's structural capacity. If the agency chooses to take an alternative action, the user may need to perform additional runs to assess the effectiveness of such actions at meeting each module's criteria. For instance, if the SG bearing capacity is inadequate to accommodate an SHL-vehicle movement, a mitigation strategy with a steel plate is an alternative option to decrease the stresses applied on top of the SG. However, users need to determine an appropriate steel-plate thickness to decrease the stresses on top of the SG to an acceptable level. This process

may involve trial and error, and the user must consider appropriate assumptions about the bonding conditions between a steel plate and the existing pavement surface layer.

1.4. ANALYSIS ENGINE COMPONENT

Pavement responses (i.e., stresses, strains, and displacements) are essential to evaluating pavement performance and serviceability under SHL-vehicle movements. Since almost all the A and B modules rely on pavement responses, it is efficient to have a single analysis engine for calculating pavement responses instead of individual built-in functions for each module. As mentioned in section 1.1, this analysis engine is called 3D-Move ENHANCED, and the model is based on the original formulation developed by Siddharthan et al.[10–12] A number of enhancements were incorporated into the original formulation, primarily with respect to the method of calculating responses, interface bonds, and runtime improvements.[10]

3D-Move ENHANCED inherited a number of unique features from its original formulation.[10,12] Notably, 3D-Move ENHANCED performs all of the associated calculations in the frequency domain using a fast Fourier transform (FFT) algorithm. For instance, since 3D-Move ENHANCED employs a two-dimensional (2D) Fourier transform to describe SHL-vehicle axles, pavement–tire interaction stresses can be nonuniform and any shape. 3D-Move ENHANCED calculations are independent for each Fourier wave. Thus, a parallel processing scheme was incorporated with the 3D-Move ENHANCED formulation in order to significantly improve the runtime.[10,13] Viscoelastic materials (e.g., asphalt mixture) could be characterized based on 3D-Move ENHANCED formulation. More importantly, 3D-Move ENHANCED considers the influence of pavement temperature and speed of the SHL vehicle on the modulus of viscoelastic material(s) used in pavement layers that exhibit such characteristics. Since SHL vehicles typically operate at slow speeds, they are anticipated to cause additional pavement damage when compared to such vehicles traversing the pavement at higher speeds. Therefore, consideration of the lower vehicle speed is important for realistic assessment of the impact of SHL-vehicle movements on flexible pavements.

From a computer-programming prospective, the formulation of 3D-Move ENHANCED is complex to implement as a single computer package. For instance, the formulation contains 2D forward and inverse FFT, as well as substantial matrix calculations. Thus, a number of different computer-programming languages were scrutinized to evaluate whether they supported such features as well as other features like stand-alone execution, GUI, and the capability to support convenient cross connections or tie-ins between SuperPACK components, mainly the connection between 3D-Move ENHANCED and the A or B modules. Matrix Laboratory (MATLAB) was selected because it supports 2D Fourier transform and handles large matrix manipulations efficiently.[14] MATLAB facilitates the development of GUI programs that can be implemented as individual functions. These features are suited to the development of SuperPACK because MATLAB helps link different SuperPACK components reliably together, as well as with the SuperPACK main window. In addition to these MATLAB features, a MATLAB code can be compiled and published as a stand-alone software package. Researchers used this feature to make SuperPACK so all interested users can download and run it on their personal computers. A MATLAB runtime complier is needed to run SuperPACK, which is available for free online. As a result, MATLAB was selected as the programming language to develop SuperPACK and its associated components (i.e., the main GUI, A and B modules, and 3D-Move ENHANCED).[14,10]

Since SuperPACK contains modules, each of which requires an individual GUI, the ties between them, 3D-Move ENHANCED, and the SuperPACK main window have been effectively handled by MATLAB. The details of 3D-Move ENHANCED, including formulation and enhancements relative to the original 3D-Move formulation, are presented in chapter 2.

1.5. SUMMARY

In this chapter, SuperPACK has been introduced as a practical software package to analyze specific cases of SHL-vehicle movements. SuperPACK contains the main GUI, five A and five B modules, and 3D-Move ENHANCED. The modules are accessible to the user through the main window, where the user first inputs general information for pavement structure and material types and subsequently proceeds to the A and then B modules. These modules may need values of specific pavement responses, which are provided by the built-in analysis engine, 3D-Move ENHANCED. Although the user does not directly interact with 3D-Move ENHANCED, most of the A and B modules tie to it internally to obtain necessary pavement responses to conduct the analysis of interest.

The MATLAB programming language was selected and used to develop SuperPACK because it has unique capabilities like offering a compiling option to have a stand-alone program, featuring easy-to-use GUI, and supporting straightforward connections between different SuperPACK components.[14] From a computational prospective, MATLAB supports 2D forward and inverse Fourier transform, as well as intensive matrix calculations associated with 3D-Move ENHANCED formulation.[14,10]

CHAPTER 2. 3D-MOVE ENHANCED

2.1. INTRODUCTION

Reliable estimation of pavement responses is important when pavement mechanistic–empirical (ME) models are to be used. Typically, ME models use pavement responses to predict major distresses, such as fatigue cracking and rutting. These distresses adversely affect pavement performance. Thus, a better estimation of pavement responses leads to a better prediction of those pavement distresses. In ME models, pavement distresses are correlated to one or more pavement responses. For instance, fatigue cracking is correlated with tensile strain at the bottom of an asphalt concrete (AC) layer in the *Guide for Mechanistic–Empirical Pavement Design of New and Rehabilitated Pavement Structures*.[15] Reliable estimation of pavement responses significantly contributes to realistic prediction of pavement performance. For an SHL-vehicle movement, the pavement performance and serviceability can be of concern when compared to a conventional pavement analysis under a standard (or reference) vehicle. Therefore, unreliable predictions of pavement responses under SHL-vehicle axles can lead to undependable estimations of pavement performance (e.g., fatigue life or rutting life) and pavement serviceability (e.g., pavement-surface deflection).

Early pavement mechanical-analysis models were based on multilayer linear elastic theory (MLET). For instance, VESYS, BISAR, and KENLAYER are among the popular software packages using this approach.[16–18] The main advantage of these software packages are that they are computationally efficient because the formulation is based on the presence of axisymmetric surface loads. Notable shortcomings are their inability to model noncircular moving load, nonuniform contact stress distribution (normal and shear), and viscoelastic material property.

The finite element method (FEM) has been employed to overcome some of the shortcomings associated with MLET. Accordingly, pavement-analysis software was developed based on the FEM. Specific issues, such as the influence of external boundaries and element discretization, remain. 3D-Move ENHANCED was developed as a robust pavement-response analysis model for the evaluation of SHL-vehicle movements on flexible pavements and as part of SuperPACK with the objective of overcoming limitations associated with MLET and the FEM. As noted in section 1.4, a number of enhancements were introduced to the original formulation to make it suitable for use with SuperPACK. 3D-Move ENHANCED and its predecessor, 3D-Move, use a finite layer approach and account for viscoelastic-material characterization.[11] Furthermore, the model is capable of analyzing SHL-vehicle axles moving at a constant speed with noncircular and nonuniform pavement–tire interaction stresses. The ability to model moving loads is critical because SHL vehicles operate at notably low speeds that can cause significant pavement damage. Surface shear stresses in both longitudinal and lateral directions can be modeled independently with 3D-Move ENHANCED with no limitation due to symmetry. This capacity is very important when the influence of interface shear stresses from a vehicle breaking on pavement damage is to be investigated. 3D-Move ENHANCED is also capable of providing three-dimensional (3D) surface plots for the pavement response of interest at the desired depth within the pavement structure. Additionally, layer interface conditions, such as debonding or slippage, can be modeled using 3D-Move ENHANCED. These unique features make 3D-Move ENHANCED a robust pavement-response analysis model ideally suited for incorporation within SuperPACK.

3D-Move ENHANCED is capable of computing pavement responses under an SHL vehicle and a reference vehicle moving at a constant speed on a specific pavement structure with known material properties.[10] A reference vehicle is commonly considered an 80,000-lb truck with one single-axle single-tire of 12,000 lb (steering axle) and two sets of tandem axles with dual-tires driving axles of 34,000 lb each (driving and trailer axles). SHL vehicles have gross vehicle weights of 250,000 lb or greater. There are other special considerations associated with SHL vehicles that differentiate them from the analysis of a reference vehicle used in conventional pavement design and analysis. For instance, stresses induced by an SHL vehicle can be significantly higher than those induced by a reference vehicle, and an SHL vehicle operates at significantly slower speeds. Therefore, the bearing capacity of SG soil may not be sufficient to accommodate an SHL-vehicle movement. The vertical displacement at the pavement surface can be substantially higher under SHL-vehicle axles. As a result, pavement serviceability can be at risk, and increased levels of rutting are anticipated. A direct consequence of lower vehicle speeds is lower effective moduli for layers that exhibit viscoelastic behavior (e.g., surface AC layer). This decrease results in much larger stresses in the unbound pavement layers that support the surface layer. Therefore, bearing capacity and service limit are two important analysis aspects of a specific SHL-vehicle movement. Both of these analyses necessitate pavement responses that need to be determined by 3D-Move ENHANCED. For instance, module B1 needs the vertical stress at a specific depth in the SG, which has to be provided by 3D-Move ENHANCED. On the other hand, module B2 requires the vertical surface displacements that are computed by 3D-Move ENHANCED.

In specific cases, a flexible pavement may include sloped shoulders, or buried utilities (e.g., pipes) may exist at certain depths from the pavement surface. These cases need special attention when an SHL-vehicle movement is expected. The stability of the sloped pavement shoulder, when one exists, is critical and needs to be evaluated. This analysis requires estimation of the stresses induced by the SHL vehicle at given locations within the pavement shoulder. In the special case of buried utilities, vertical stresses on top of the buried utility must be calculated to ensure that the utility does not fail. These responses must be calculated and provided by 3D-Move ENHANCED.

As mentioned in section 1.4, modules B1 through B4 require pavement responses. There are criteria associated with these modules to ensure that SHL-vehicle movement does not jeopardize pavement performance or serviceability. For instance, the bearing stress on an SG due to an SHL-vehicle movement is compared to the SG's bearing capacity to ensure that failure does not occur. The maximum vertical surface displacement caused by an SHL vehicle is compared to the allowable displacement to verify that pavement serviceability is in good standing. On the other hand, module B5 does not include any criteria. The level of damage (e.g., rutting and fatigue damage) associated with an SHL-vehicle movement is quantified in terms of dollars per lane-mile in module B5. This module is based on the pavement remaining-life concept that uses inputs, such as construction cost per lane-mile, interest rate, etc. Module B5 provides the user with the PDAC attributed to the pavement structure. Therefore, it is the user's responsibility to apply engineering judgment to see if the PDAC for the analyzed SHL-vehicle movement is reasonable or if additional analyses using different mitigation strategies are needed to decrease the PDAC. In any case, module B5 requires critical pavement responses for completing the remaining-life analysis based on rutting and fatigue cracking. The necessary pavement responses

to conduct cost allocation analysis are provided by 3D-Move ENHANCED. Details about the cost allocation method are presented in Volume IX: Appendix H.[9]

2.2. FORMULATION

The finite layer approach employed in the 3D-Move ENHANCED formulation is based on the wave-propagation concept. In this approach, each layer in the pavement structure is modeled individually as a single continuum, as opposed to the FEM, in which all the pavement layers are decomposed into many finite elements. In the finite layer approach, the surface load is decomposed into many waves that are represented in spatial and frequency domains. Displacements are considered the main unknowns in 3D-Move ENHANCED. It is assumed that displacements have the same frequency as the load for every wave. However, their amplitudes vary within the pavement structure. Details the about 3D-Move ENHANCED formulation are presented in section 2.2.1 and section 2.2.2.

2.2.1. Surface-Load Representation

Distribution of tire–pavement interaction stresses is represented as a 2D domain in *x*- and *y*-directions. This load is identified by module A1. Assuming *x*-direction is the direction of travel for the SHL vehicle, the surface stress distribution can be expressed as in figure 3.

$$p(x,y) = \sum_{m=1}^{M} \sum_{n=1}^{N} A_{mn}\, e^{i\omega_x x} e^{i\omega_y y}$$

Figure 3. Equation. Surface load representation for SHL-vehicle axles.

Where:

$p(x, y)$ = vertical stress for a point with coordinates of (x, y).
M = total number of waves in *x*-direction.
N = total number of waves in *y*-direction.
m = wave number in *x*-direction.
n = wave number in *y*-direction.
i = imaginary number.
ω_x = spatial frequency in *x*-direction.
ω_y = spatial frequency in *y*-direction.
A_{mn} = Fourier coefficient matrix, which is determined by applying a 2D FFT algorithm on the stress matrix (i.e., $p(x, y)$).

Considering the SHL vehicle is travelling at a speed (V) in *x*-direction, the modified load representation equation for speed is the equation presented in figure 4, where t is time.[11]

$$p(x,y) = \sum_{m=1}^{M} \sum_{n=1}^{N} A_{mn}\, e^{i\omega_x (x-Vt)} e^{i\omega_y y} = \sum_{m=1}^{M} \sum_{n=1}^{N} A_{mn}\, e^{i(-V\omega_x)t} e^{i\omega_x x} e^{i\omega_y y}$$

Figure 4. Equation. Surface stress representation for SHL axles modified for SHL-vehicle speed.

General Form of Displacements

As mentioned in section 2.1, displacements are the main unknowns in 3D-Move ENHANCED formulation. If the displacement field is known, then stress and strain fields are obtained by employing strain-displacement and stress–strain (constitutive) relations. Denoting displacement in *x*-, *y*-, and *z*-directions with u_1, u_2, and u_3, respectively, the general form of displacements is presented in figure 5 for each of the three directions (j = 1, 2, 3).

$$u_j(x,y,z,t) = \sum_{m=1}^{M}\sum_{n=1}^{N} \tilde{u}_j(z) e^{i\omega_x(x-Vt)} e^{i\omega_y y}$$

Figure 5. Equation. General form of displacements.

Where:

$u_j(x,y,z,t)$ = displacement in *j*-direction at location of interest.
$\tilde{u}_j(z)$ = displacement in *j*-direction at location of interest in the frequency domain.

This equation is based on the wave-propagation concept, in which $\tilde{u}_j(z)$ is a function of depth, as the waves propagate into the pavement structure.(11)

Constitutive Equations

Constitutive equations are used to obtain stresses and strains from displacements. The normal strain-displacement constitutive equation is presented in figure 6. The shear strain-displacement constitutive equation is presented in figure 7.

$$\varepsilon_{jj} = \frac{\partial u_j}{\partial j}$$

Figure 6. Equation. Normal strain-displacement constitutive equation.

Where ε_{jj} is normal strain in *j*-direction (spatial domain).

$$\varepsilon_{jk} = \frac{1}{2}\left(\frac{\partial u_j}{\partial k} + \frac{\partial u_k}{\partial j}\right)$$

Figure 7. Equation. Shear strain-displacement constitutive equation.

Where ε_{jk} is shear strain on the plane with normal strain in the *j*-direction and stretching in the *k*-direction (spatial domain).

To obtain stresses, the constitutive relationships are used. For the one-dimensional case, the stress–strain relationship is simply represented by the well-known Hook's law. However, in the 3D case, the normal stress–strain relationship is presented in figure 8.

$$\sigma_{jj} = \lambda \cdot tr(\varepsilon) + 2G \cdot \varepsilon_{jj}$$

Figure 8. Equation. Normal stress–strain constitutive equation in spatial domain.

Where:

σ_{jj} = normal stress in *j*-direction (spatial domain).
λ = first Lamé parameter.
G = second Lamé parameter.
tr(.) = field trace function (summation).

G is equal to shear modulus. In frequency domain, this equation is the equation presented in figure 9.

$$\tilde{\sigma}_{jj} = \lambda \cdot tr(\tilde{\varepsilon}) + 2G \cdot \tilde{\varepsilon}_{jj}$$

Figure 9. Equation. Normal stress–strain constitutive equation in frequency domain.

Where:

$\tilde{\sigma}_{jj}$ = normal stress in *j*-direction (frequency domain).
$\tilde{\varepsilon}$ = strain tensor (frequency domain).
$\tilde{\varepsilon}_{jj}$ = normal strain in *j*-direction (frequency domain).

Applying the strain-displacement value derived earlier, one can develop a normal stress-displacement constitutive equation. To derive a shear stress-displacement constitutive equation, the shear strain-displacement equation developed earlier (figure 7) should be coupled with the shear stress–strain equation, which leads to the equation presented in figure 10.

$$\sigma_{jk} = G\left(\frac{\varepsilon_{jk}}{2} + \frac{\varepsilon_{kj}}{2}\right)$$

Figure 10. Equation. Shear stress–shear strain constitutive equation.

Where:

σ_{jk} = shear stress on the plane with normal in the *j*-direction and stretching in the *k*-direction (spatial domain).
ε_{kj} = shear strain on the plane with normal in the *k*-direction and stretching in the *j*-direction (spatial domain).

Solution Scheme

The equation of equilibrium of forces for an arbitrary element in a pavement structure and for a specific wave is presented in figure 11.

$$\frac{\partial \sigma_{jk}}{\partial k} = \rho \frac{\partial^2 u_j}{\partial t^2}$$

Figure 11. Equation. Equilibrium equation.

Where ρ is material density.

Rearranging this equation using stress-displacement constitutive equations leads to a system of differential equations with three equations and three unknowns (displacements in three

directions). Figure 12 presents the solution for the system of equations obtained for displacement in the frequency domain and for the specific wave of interest.

$$\tilde{u}_j = A_{1j}e^{n_1 z} + A_{2j}e^{n_2 z} + A_{3j}e^{-n_1 z} + A_{4j}e^{-n_2 z}$$

Figure 12. Equation. Solution for displacements in frequency domain.

Where:

A_{1j} to A_{4j} = unknown displacement coefficients for each pavement layer.
n_1 = first eigenvalue for the pavement system, as shown in figure 13.
n_2 = second eigenvalue for the pavement system, as shown in figure 14.

$$n_1 = \sqrt{\omega_x^2 + \omega_y^2 - \frac{\rho(\omega_x \cdot V)^2}{\lambda + 2G}}$$

Figure 13. Equation. First eigenvalue for the pavement system.

$$n_2 = \sqrt{\omega_x^2 + \omega_y^2 - \frac{\rho(\omega_x \cdot V)^2}{G}}$$

Figure 14. Equation. Second eigenvalue for the pavement system.

Among the layer displacement coefficients A_{1j} to A_{4j}, only six are independent per layer. These layer coefficients are determined based on the boundary (top and bottom) and layer interface conditions as described in the following paragraphs. After calculating displacements, stresses and strains would be calculated using stain-displacement and constitutive equations.

Boundary and Layer Interface Conditions

Boundary and layer interface conditions are employed to obtain the unknown layer coefficients to use with the equation presented in figure 12. There are three types of conditions: surface boundary, interface, and bottom boundary. For a pavement structure composed of a number of layers (N_L), there are three surface boundary conditions, $6(N_L - 1)$ interface boundary conditions, and three bottom boundary conditions for each individual wave. Therefore, there are $6N_L$ boundary conditions that may be used to find the associated coefficients for every layer ($6N_L$ unknowns).

Surface boundary conditions are, in terms of vertical normal stresses and shear stresses (in both longitudinal and lateral directions), applied to the pavement surface. A representation of surface normal stress can be found in the equation presented in figure 3. The same representations could be used for longitudinal and lateral shear stresses.

For fully bonded layers, the interface conditions would be the equality of stresses and displacements for the upper and lower layers at their interface. There are three equilibrium equations and three continuity equations at each layer interface. Figure 15 and figure 16 present the equilibrium and continuity equations, respectively.

$$\tilde{\sigma}_{jz}^{-}(\omega_x, \omega_y, H) = \tilde{\sigma}_{jz}^{+}(\omega_x, \omega_y, 0)$$

Figure 15. Equation. Equilibrium equation for layer interface boundary conditions.

Where:

$\tilde{\sigma}_{jz}^{-}(\omega_x, \omega_y, H)$ = stress at the bottom of the upper layer.
$\tilde{\sigma}_{jz}^{+}(\omega_x, \omega_y, 0)$ = stress at the top of the lower layer.
H = thickness of the upper layer.

$$\tilde{u}_j^{-}(\omega_x, \omega_y, H) = \tilde{u}_j^{+}(\omega_x, \omega_y, 0)$$

Figure 16. Equation. Continuity equation for layer interface boundary conditions.

Where:

$\tilde{u}_j^{-}(\omega_x, \omega_y, H)$ = displacement in *j*-direction at the bottom of the upper layer.
$\tilde{u}_j^{+}(\omega_x, \omega_y, 0)$ = displacement in the *j*-direction at top of the lower layer.

All parameters used in this equation are in the frequency domain for a specific wave with spatial frequencies of ω_x and ω_y in the *x*- and *y*-direction, respectively.

Bottom boundary conditions are considered no displacement at a certain depth of the last layer. The equation for bottom boundary condition is presented in figure 17.

$$\tilde{u}_j(\omega_x, \omega_y, H_N) = 0$$

Figure 17. Equation. Three bottom boundary conditions.

Where H_N is location of the bottom boundary with respect to the last layer interface.

Viscoelastic Material Characterization

One of the unique features for 3D-Move ENHANCED inherited from the original 3D-Move formulation is the viscoelastic material characterization. Since the formulation is based on Fourier transform, the frequency of each wave could be used to obtain the corresponding elastic modulus of viscoelastic material, such as AC. Based on the equation presented in figure 4, time frequency of loading may be calculated using the equation presented in figure 18.

$$\omega_t = -\omega_x \cdot V$$

Figure 18. Equation. Time frequency of loading for viscoelastic material characterization.

Recalling that V is the speed of the SHL vehicle and ω_x is the spatial frequency for the wave of interest in *x*-direction, the angular frequency (ω_t) may be used with an AC modulus master curve or a mechanical model (e.g., Kelvin model, Maxwell model, and Burger model) to determine the viscoelastic material modulus for the wave of interest. Knowing that the effect of pavement temperature is included in the elastic modulus master curve, the pavement temperature and SHL-vehicle speed are taken into consideration in the formulation of 3D-Move ENHANCED.

2.2.2. Enhancements to 3D-Move Analysis

The basis for the 3D-Move ENHANCED formulation is described in section 2.2.1. This section presents the following three main enhancements that were incorporated as part of this formulation: generating surface plots, interface bond conditions, and runtime improvement.

Surface Plots

In the original 3D-Move formulation, pavement mechanical responses were calculated for a specific point within the pavement structure by a summation of responses from all the waves in *x*- and *y*-directions. However, in the new formulation, an inverse Fourier transform was employed to obtain surface plots for pavement responses at a specific depth. In this method, the respective response for each wave is first calculated in the frequency domain. Then, the response is transformed into the spatial domain using the inverse Fourier algorithm. These methods can be applied for all 15 responses (i.e., 3 displacements, 6 stresses, and 6 strains). The surface plot of responses can be generated for a particular time step of analysis. As an example, the top and perspective views for a sample SHL-vehicle quad axle are presented in figure 19 and figure 20. The vertical surface displacement under this SHL-vehicle quad axle traveling at a low constant speed is presented in figure 21 as a 3D surface plot.

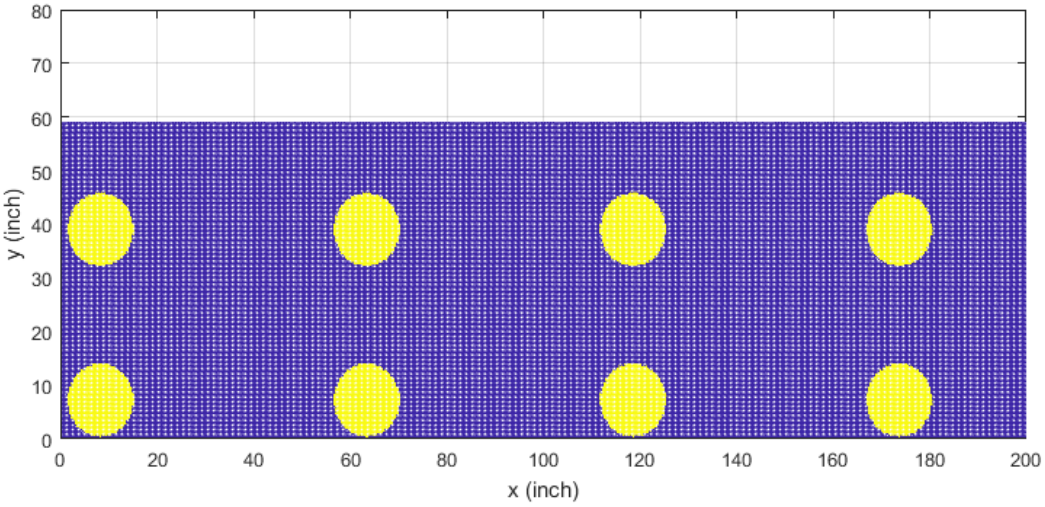

Figure 19. Graph. Sample of SHL-vehicle quad axle (top view).

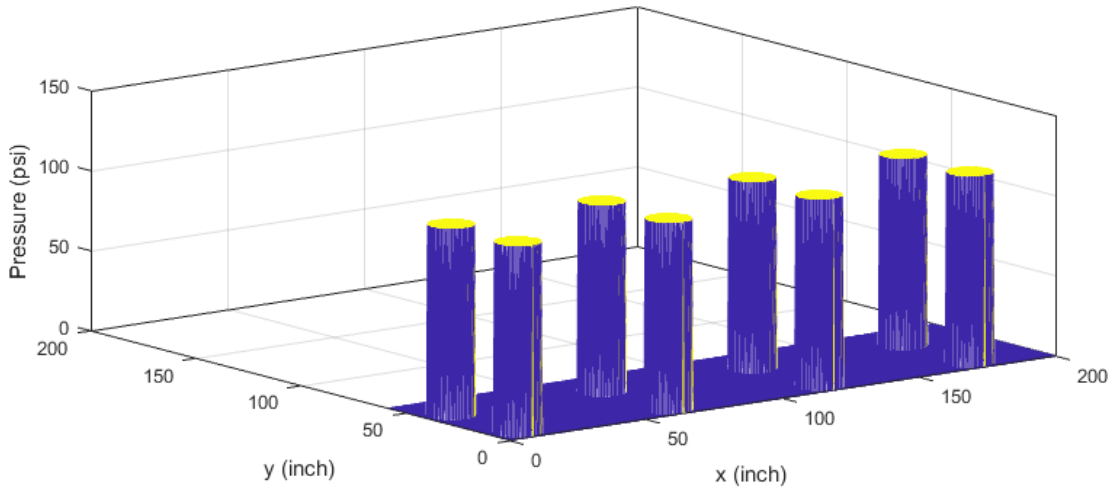

Figure 20. Graph. Sample of SHL-vehicle quad axle (perspective view).

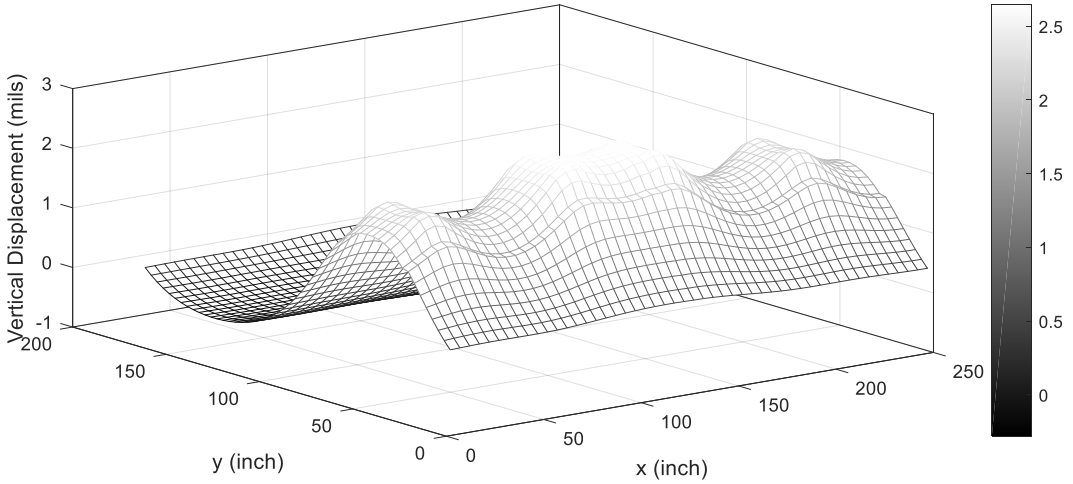

Figure 21. Graph. Surface plot for vertical displacement at pavement surface under a sample SHL-vehicle quad axle.

Interface Bond Conditions

Interface debonding is a significant issue in pavement remediation (i.e., mitigation), which involves layer-to-layer interaction at the interface. This issue can be critical for pavements subjected to large loading, such as SHL vehicles and aircrafts. Sometimes mitigation strategies such as steel plates are used to decrease the detrimental effects of an SHL-vehicle movement. In this case, the steel plates and existing pavement surface layer do not represent fully bonded conditions. Therefore, proper modeling of the layer bond condition is essential for flexible pavements subjected to an SHL-vehicle movement. Layer interface debonding was incorporated into SuperPACK through 3D-Move ENHANCED.[10]

The analytical approach adopted in 3D-Move ENHANCED, particularly the formulation of interface boundary conditions, allows for effective incorporation of various interface bond condition models.[10] There have been several methods suggested in the literature to model slippage or debonding at layer interfaces. However, a modified version of the slippage model developed by Maina et al. was used to model interface bond conditions.[19] The modified equations for interface layer boundary conditions are presented in figure 22 and figure 23 for *x*- and *y*-directions, respectively.

$$u_1^-(H_i) - \tilde{u}_1^+(0) = \frac{\tau_{xz}^i(H_i)}{K_{xx}}$$

Figure 22. Equation. Modified layer interface boundary conditions to include interface bond conditions in *x*-direction.

Where:

$u_1^-(H_i)$ = displacements in *x*-direction at the bottom of layer *i*.
$\tilde{u}_1^+(0)$ = displacements in x-direction at the bottom of layer (*i* + 1).
$\tau_{xz}^i(H_i)$ = longitudinal shear stresses at the interface of layers *i* and (*i* + 1).
K_{xx} = shear slippage stiffness in *x*-direction.

$$u_2^-(H_i) - \tilde{u}_2^+(0) = \frac{\tau_{yz}^i(H_i)}{K_{yy}}$$

Figure 23. Equation. Modified layer interface boundary conditions to include interface bond conditions in *y*-direction.

Where:

$u_2^-(H_i)$ = displacements in *y*-direction at the bottom of layer *i*.
$\tilde{u}_2^+(0)$ = displacements in *y*-direction on top of layer (*i* + 1).
$\tau_{yz}^i(H_i)$ = lateral shear stresses at the interface of layers *i* and (*i* + 1).
K_{yy} = shear slippage stiffness in *y*-direction.

In these equations, the formulation is provided for the interface of layers *i* and (*i* + 1). The layer closest to the pavement surface is numbered as 1, and the layer number increases with increasing depth.

Runtime Improvement

As mentioned in the introduction of this chapter, MATLAB was used to develop SuperPACK and associated components, including 3D-Move ENHANCED.[14,10] Most processing time for the different modules is consumed in computing pavement responses. Therefore, improving the runtime of 3D-Move ENHANCED would significantly improve the runtime for SuperPACK. In this respect, employing an inverse Fourier transform helped significantly decrease runtime compared to the original approach for computing response points using a summation of all responses from all waves. Not only is the new approach substantially quicker than the original approach, it also generates plots for different responses at any given horizontal plane within the pavement structure.

Another mechanism used to improve runtime was parallel processing. In fact, formulation of 3D-Move ENHANCED allows for parallel processing because the responses from the waves are processed independently.[10] Therefore, values for response(s) of interest could be determined by assigning waves to different processing units. Responses in the frequency domain are collected from all processing units and assembled. Pavement responses are transformed into the space domain using inverse Fourier transform. The speed-up factor was close to 3 for a quad processor (75-percent increase in speed-up factor), showing that the parallel process can efficiently improve the runtime of 3D-Move ENHACNED. Table 2 summarizes the runtime in seconds for 3D-Move Enhanced considering parallel processing for a single layer and up to 10 pavement layers.

Table 2. Runtime for 3D-Move ENHANCED considering parallel processing.

N_L	Runtime (Seconds)
1	11
2	22
3	33
4	45
5	56
6	67
7	79
8	90
9	102
10	115

2.3. SUMMARY

This chapter has presented the formulation of 3D-Move ENHANCED, which provides pavement responses needed for the A and B modules. Pavement responses are computed for an SHL-vehicle traveling at a specific speed. The formulation is based on the finite layer approach, which is based on the concept of wave propagation. The surface load is represented as a composition of waves traveling in *x*- and *y*-directions using a 2D FFT. Subsequently, all the calculations are performed in the frequency domain. The main unknowns for 3D-Move ENHANCED are displacements in the three directions. Stresses and strains are calculated based on displacements using stress- and strain-displacement constitutive equations, respectively. 3D-Move ENHANCED is capable of modeling viscoelastic material behavior.

Enhancements were made to the original 3D-Move formulation in the development of 3D-Move ENHANCED.[10,12] These modifications included generating surface plots of responses, interface bond conditions that allow for slippage, and runtime improvement through parallel processing. Because inverse Fourier transform is employed in 3D-Move ENHANCED, surface plots for a particular response could be obtained at the desired depth within the pavement structure. Since SuperPACK runtime relies on pavement responses, 3D-Move ENHANCED is a significant improvement. Parallel processing was incorporated into the formulation as waves associated with pavement responses can be processed independently.

CHAPTER 3. SuperPACK

3.1. INTRODUCTION

SuperPACK can be used to evaluate a specific SHL-vehicle movement case. As mentioned in the previous chapter, SuperPACK was programmed in MATLAB because MATLAB has the GUI feature and efficient support of matrix calculations needed for 3D-Move ENHANCED.[14,10]

SuperPACK is composed of three main components: five A and five B modules and an analysis engine. The A modules are explained in section 3.2, and the B modules are explained in section 3.3. The A and B modules are accessed from the SuperPACK main window (figure 2). Completion of the A modules is a prerequisite for proceeding to the B modules. The user should enter the information needed for calculating pavement responses (e.g., pavement structure and material types) in the main window. The pavement responses needed for particular A or B modules are provided by 3D-Move ENHANCED. Each time a module requires a pavement response for its assigned calculations, it has to make a connection to 3D-Move ENHANCED and requests the response type and depth (or point) of interest. In addition to inputs provided by 3D-Move ENHANCED (i.e., pavement responses), each of the A and B modules has a GUI to input user data for that specific module. Additionally, some modules may need data from other modules. Likewise, an A module may need the user to provide information in the main window. Figure 24 schematically presents different SuperPACK components and their interactions.

3.2. A MODULES: PREANALYSIS

Section 1.2 lists the five A modules. To illustrate how these modules work, the inputs and outputs associated with modules A1 through A5 are presented in table 3 through table 7, respectively. All of the A modules should be processed by the user to proceed to the B modules.

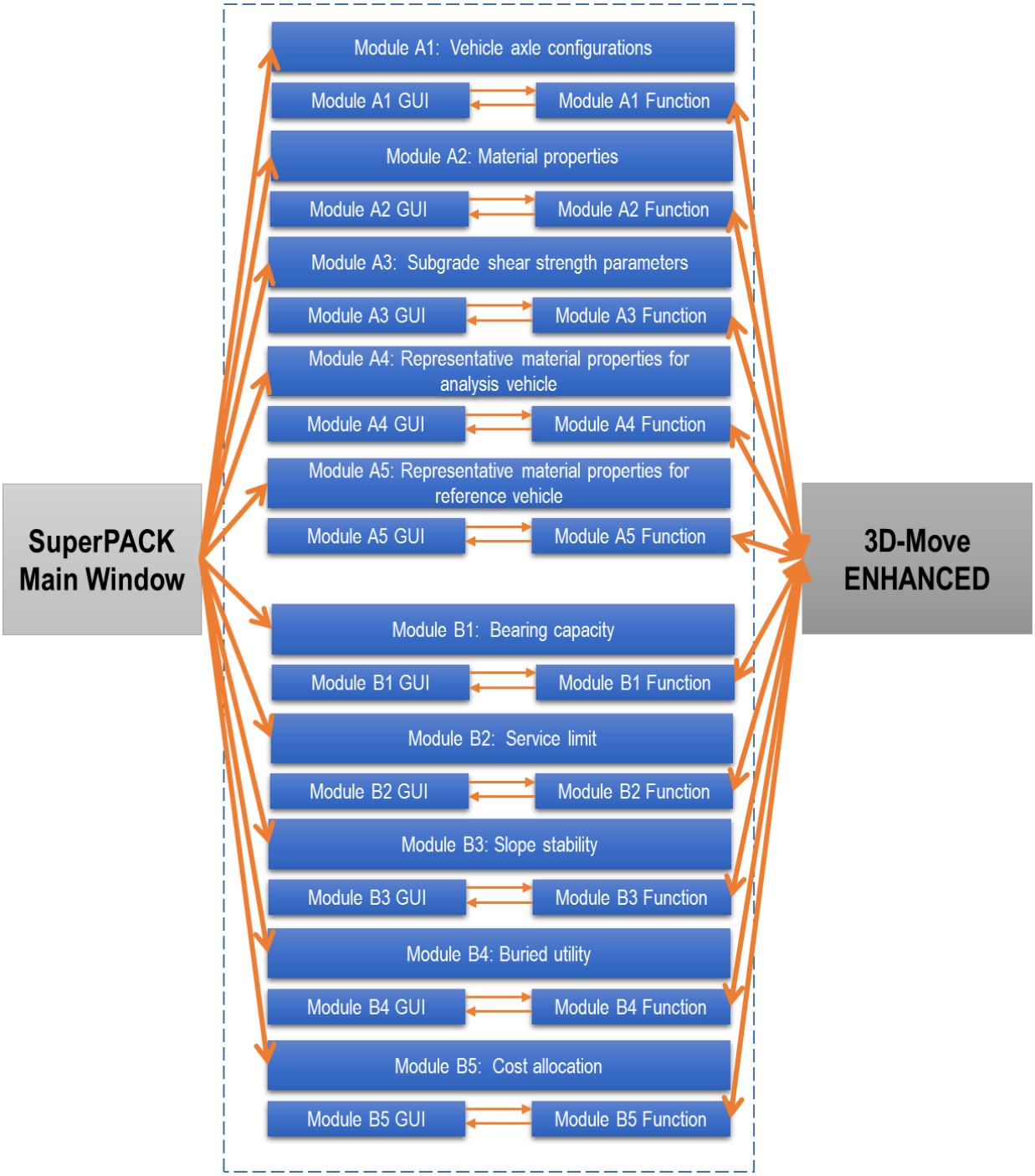

Figure 24. Illustration. SuperPACK components interaction.

Table 3. Inputs and outputs for module A1: Vehicle axle configurations.

Inputs	Outputs
1. Pavement structure. 2. Total number of axles. 3. Axle loads. 4. Spacing between the axles. 5. Number of tires for each axle. 6. Spacing between the tires for each axle.	1. Axle groups.

Table 4. Inputs and outputs for module A2: Material properties.

Inputs	Outputs
1. Pavement structure. 2. FWD plate's diameter. 3. Applied FWD-load levels. 4. Backcalculated layers' moduli at different load levels. 5. Layers' unit weight. 6. V_a content of existing AC-layer mixture. 7. V_{beff} of existing AC-layer mixture. 8. Cumulative percent retained on the ¾ sieve of existing AC-layer mixture. 9. Cumulative percent retained on the ⅜ sieve of existing AC-layer mixture. 10. Cumulative percent retained on the No. 4 sieve of existing AC-layer mixture. 11. Percent passing the No. 200 sieve of existing AC-layer mixture. 12. Binder shear modulus at multiple temperatures. 13. Binder phase angle at multiple temperatures. 14. Temperature in Rankine at which the viscosity was estimated.	1. Field-damage E^* master curve for existing AC-layer mixture. 2. M_R relationship for the base. 3. M_R relationship for the SG.

V_a = air void; V_{beff} = effective binder content; No. = number; M_R = resilient modulus; E^* = dynamic modulus.

Table 5. Inputs and outputs for module A3: SG τ_{max} parameters.

Inputs	Outputs
1. Pavement structure. 2. FWD plate's diameter. 3. Applied FWD-load levels. 4. Radial distances for FWD measurements. 5. Surface deflection at different radial distances. 6. Backcalculated layers' moduli at different load levels. 7. Layers' unit weight. 8. Representative range for the SG friction angle.	1. Stress dependency using load-response characteristic method. 2. Stress dependency using deflection ratio method. 3. Estimation of the SG τ_{max} parameters.

Table 6. Inputs and outputs for module A4: Representative material properties for analysis vehicle.

Inputs	Outputs
1. Pavement structure. 2. FWD plate's diameter. 3. Applied FWD-load levels. 4. Backcalculated layers' moduli at different load levels. 5. Layers' unit weight. 6. Standard truck axle configuration. 6.1. Axle spacing. 6.2. Tire spacing. 6.3. Tire pressure. 6.4. Tire loading. 7. Standard truck speed. 8. Field damage E^* master curve for existing AC-layer mixture. 9. Analysis temperature. 10. M_R relationship for the base. 11. M_R relationship for the SG.	1. Representative material properties under standard truck. 1.1. M_R of the base layer. 1.2. M_R of the SG layer.

E^* = dynamic modulus; M_R = resilient modulus.

Table 7. Inputs and outputs for module A5: Representative material properties for reference vehicle.

Inputs	Outputs
Pavement structure. 1. Layers' unit weight. 2. SHL-vehicle axle configuration. 2.1. Axle spacing. 2.2. Tire spacing. 2.3. Tire pressure. 2.4. Tire loading. 3. SHL truck speed. 4. Field damage E^* master curve of existing AC-layer mixture. 5. Analysis temperature. 6. M_R relationship for the base. 7. M_R relationship for the SG. 8. Material properties under standard truck. 8.1. M_R of the base layer. 8.2. M_R of the SG layer. 9. Depth of interest for identifying the nucleus.	1. Influential number of tires in x-direction. 2. Influential number of tires in y-direction. 3. Representative nucleus of axle load configuration. 4. Representative material properties under the SHL-vehicle nucleus. 4.1. M_R of the base layer. 4.2. M_R of the SG layer.

E^* = dynamic modulus; M_R = resilient modulus.

3.2.1. Module A1: Vehicle Axle Configurations

Because SHL vehicles typically have large dimensions and may occupy more than one lane, one single pavement analysis for the entire SHL vehicle may not be possible due to a high computational effort. Accordingly, the SHL vehicle is decomposed into different axle groups, and those groups are analyzed independently. This analysis relies on the fact that a response at a particular depth within the pavement structure due to an axle group is not influenced by other groups. Pavement analysis is performed for all axle groups, and the needed critical responses are

used in the calculations by the respective modules. Inputting SHL-vehicle axle configuration and decomposing it into different groups of axles is the task of module A1. More details on determining vehicle axle groups are presented in Volume III: Appendix B.(3)

Figure 25 illustrates the developed GUI for module A1. As an example, the axle configuration for a sample SHL vehicle is identified in this module. A sample SHL-vehicle axle configuration and spacing, as well as axle load, are presented in figure 26. The SHL vehicle has a total of 10 axles.

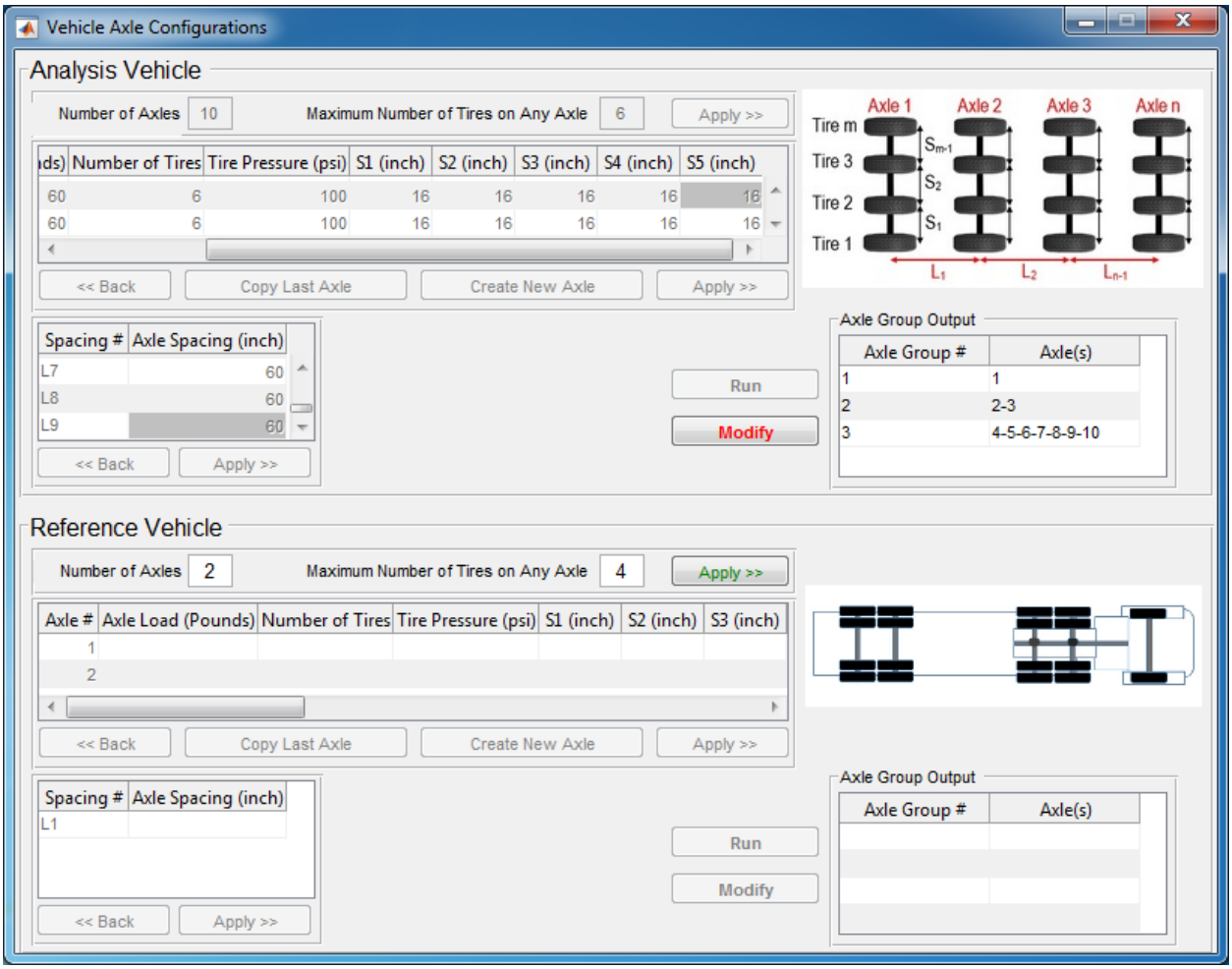

© 2018 UNR.

Figure 25. Screenshot. Module A1: vehicle axle configurations.

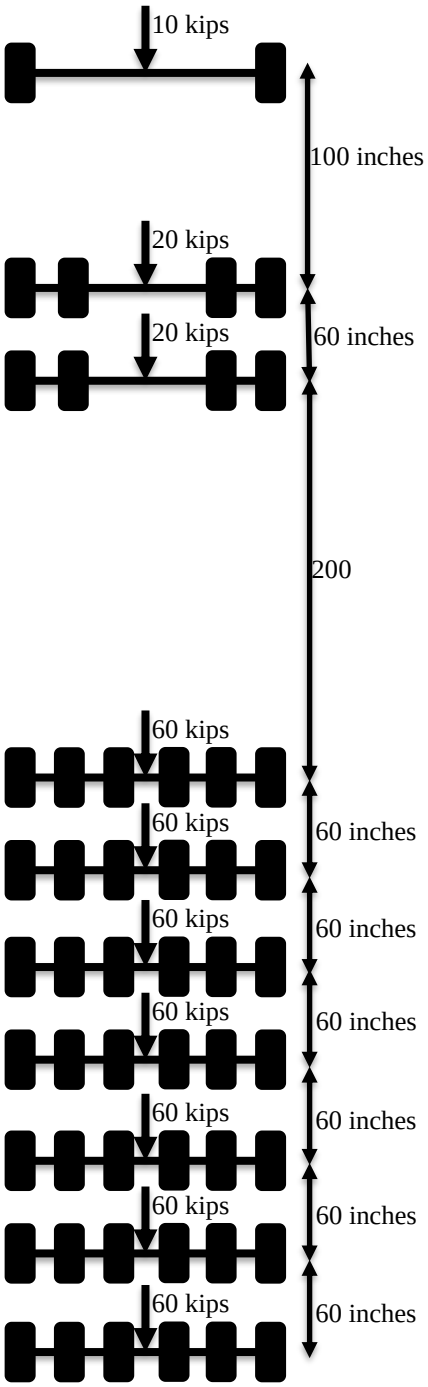

Figure 26. Sketch. Sample SHL vehicle.

3.2.2. Module A3: SG τ_{max} Parameters

SG shear strength parameters c and ϕ are essential for analyzing an SHL-vehicle movement. These parameters are needed in modules B1 through B3. Details about the calculations included in these modules are presented in Volume IV: Appendix C.[4] Module A3 requires FWD

backcalculation data in order to calculate SG shear strength parameters. Backcalculation data should be entered by the user in the SuperPACK main window before running this module (figure 2). If FWD backcalculation data are not available, the user can manually input values for c and ϕ. These values could be obtained from laboratory measurements on SG samples or specified based on the user's engineering judgment.

Figure 27 presents the developed GUI for module A3. In the top panel portion, "Range of Friction Angle," the user should input soil classification based on the Unified Soil Classification System. Thereafter, the accepted ranges for minimum and maximum ϕ need to be entered. The user has the option to change these values. After clicking "Run," the c-ϕ plot and average values for c and ϕ are presented to the user in the "Estimated Shear Strength Parameters" panel. The estimated shear strength parameters can be overwritten by the user in the "Overwrite Shear Strength Parameters" panel. In this panel, the user inputs ϕ, and c would be updated accordingly.

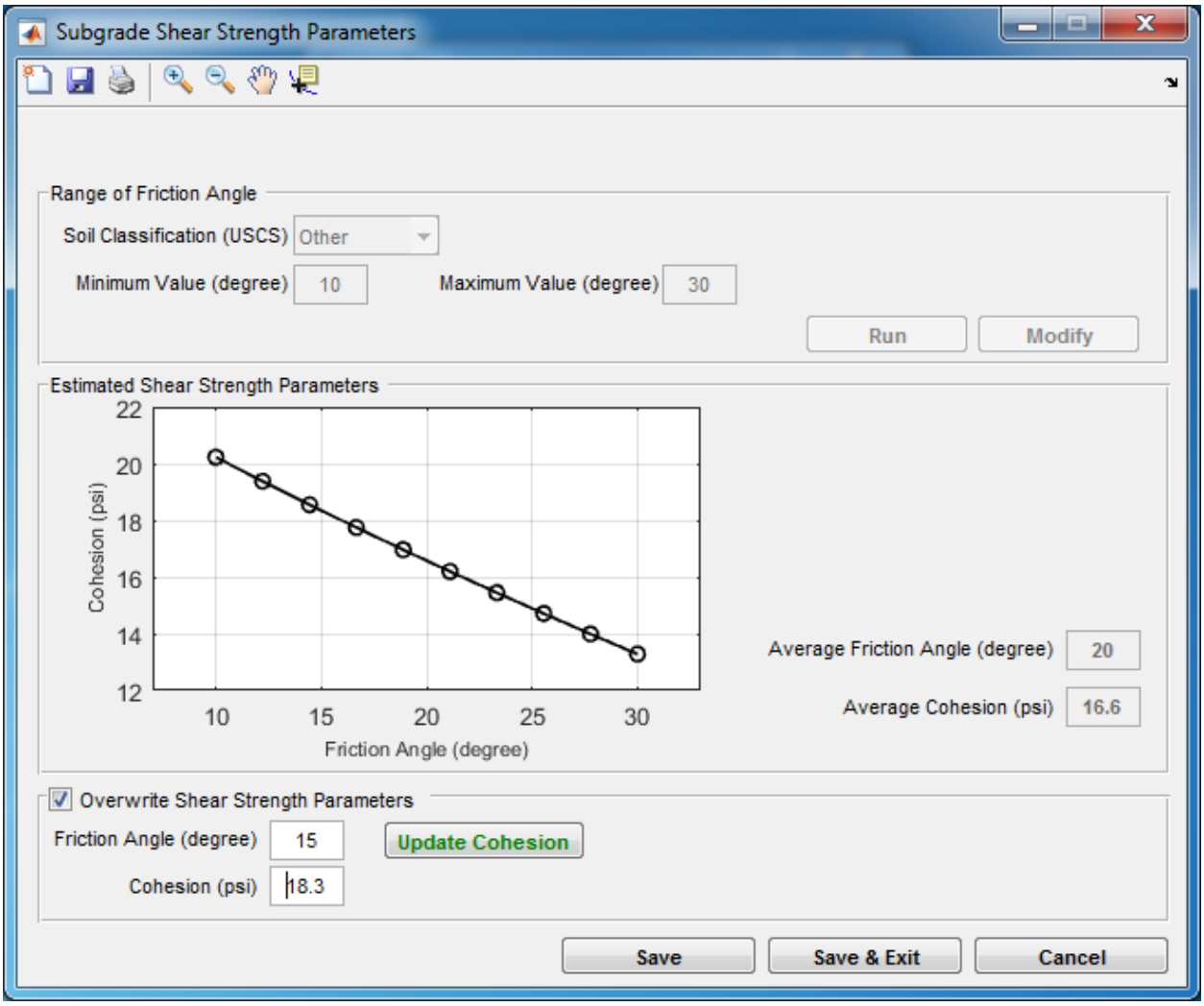

USCS = Unified Soil Classification System.

Figure 27. Screenshot. Module A3: SG shear strength parameters.

3.2.3. Module A4: Representative Material Properties for Analysis Vehicle

Figure 28 features the GUI for module A4. In this figure, SHL-vehicle axle configurations are presented in the "Analysis Vehicle Axle Configuration" panel. Information in this panel is retrieved from module A1 so that the user can visualize it. After clicking "Run" in the same panel, the most critical axle group number that induces the highest vertical stress at the depth of 6 inches below the SG surface is reported in the "Analysis Vehicle Critical Axle Group." The nucleus representing the critical axle group is also presented in the "Nucleus of Critical Axle Group" panel.

The "Nucleus of Critical Axle Group" presents two main plots: tire nucleus with obtained number of additional tires in *x*- (N_x) and *y*-directions (N_y), respectively, and normalized vertical stress as a function of number of tires. The "Representative Material Properties" panel contains the representative resilient modulus (M_R) values for stress-dependent layers. The stress-dependent layers must be selected by the user in the main window before running module A4.

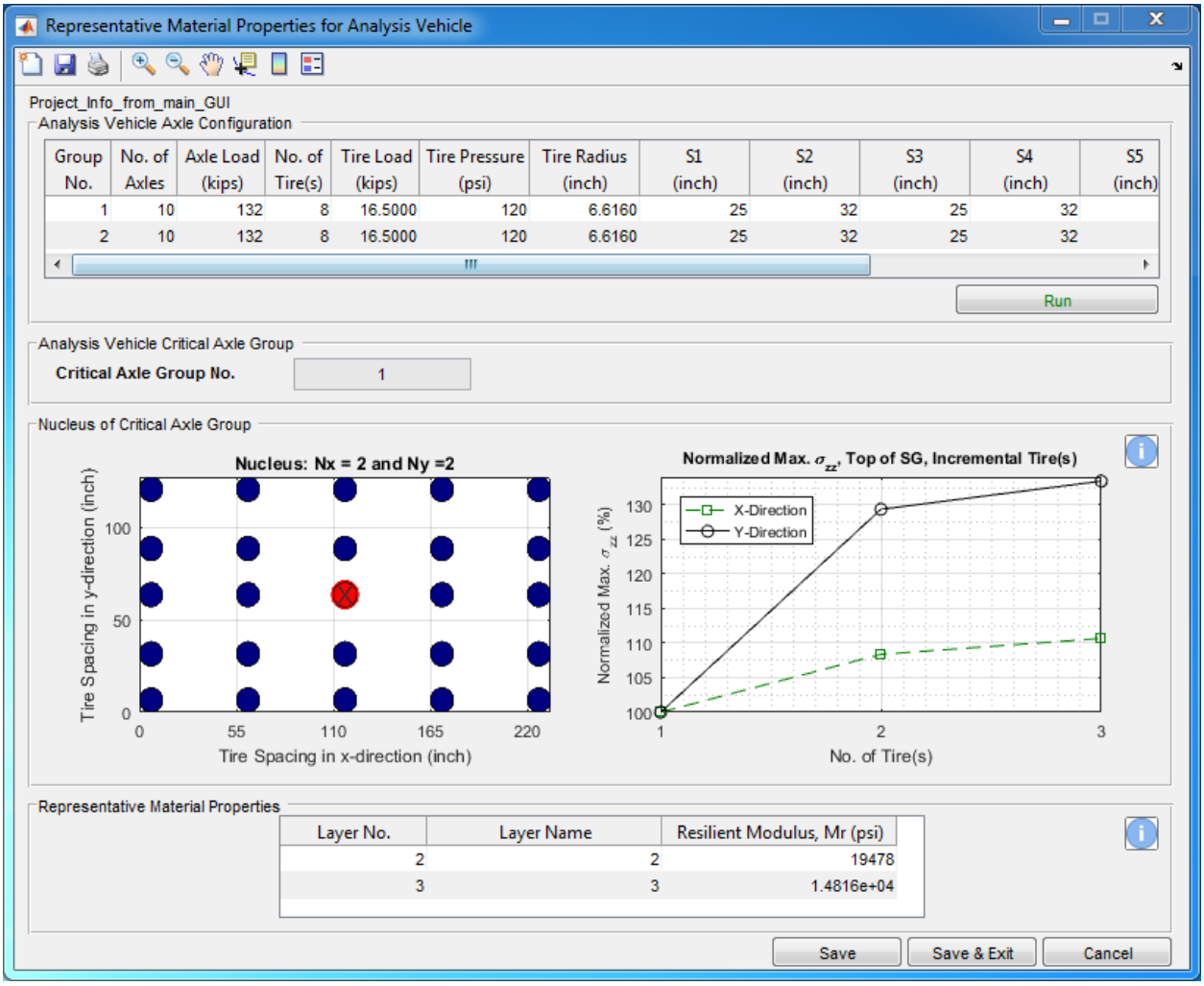

Figure 28. Screenshot. Module A4: Representative material properties for analysis vehicle.

3.3. B MODULES: ANALYSIS

Section 1.3 lists the five B modules. Elements of module B5 are explained in section 3.3.1. The B modules can be accessed through the SuperPACK main window (figure 2) and are active after the A modules have been completed. Table 8 through table 12 present the inputs and outputs of modules B1 through B5, respectively.

Table 8. Inputs and outputs for module B1: Bearing capacity.

Inputs	Outputs
1. Pavement structure. 2. Representative nucleus of SHL-vehicle configuration. 2.1. Axle spacing. 2.2. Tire spacing. 2.3. Tire pressure. 2.4. Tire loading. 3. SHL truck speed. 4. Field damage E^* master curve of existing AC-layer mixture. 5. Analysis temperature. 6. Material properties under SHL truck. 6.1. M_R of the base layer. 6.2. M_R of the SG layer. 7. Estimated SG τ_{max} parameters.	1. Maximum average stress on top of the SG using representative nucleus of SHL-vehicle configuration. 2. q_u of the SG layer. 3. FOS against general bearing capacity failure of the SG layer and the need for mitigation strategy.

E^* = dynamic modulus; q_u = ultimate bearing capacity; FOS = factor of safety.

Table 9. Inputs and outputs for module B2: Service limit.

Inputs	Outputs
1. Pavement structure. 2. Representative nucleus of SHL-vehicle configuration. 2.1. Axle spacing. 2.2. Tire spacing. 2.3. Tire pressure. 2.4. Tire loading. 3. SHL truck speed. 4. Field damage E^* master curve of existing AC-layer mixture. 5. Analysis temperature. 6. Material properties under SHL truck. 6.1. M_R of the base layer. 6.2. M_R of the SG layer. 7. Estimated SG τ_{max} parameters. 8. Standard truck axle configuration. 8.1. Axle spacing. 8.2. Tire spacing. 8.3. Tire pressure. 8.4. Tire loading. 9. Standard truck speed. 10. Material properties under standard truck. 10.1. M_R of the base layer. 10.2. M_R of the SG layer. 11. FWD plate's diameter. 12. Applied FWD-load levels. 13. Backcalculated moduli at different load levels. 14. Surface deflection at center of loading plate. 15. Layers' unit weight.	1. Equivalent triaxial state of stresses under nucleus of SHL-vehicle configuration at the top of SG. 2. FOS against the localized shear failure and the need for mitigation strategy. 3. Stress level under FWD loading and the nucleus of SHL-vehicle configuration at the top of SG. 4. FWD_{equiv} corresponding to the SHL using the computed stress level. 5. Surface deflection under the nucleus of SHL-vehicle configuration. 6. Comparison of the surface deflection under the nucleus of SHL configuration with FWD measurements. 7. FWD_{equiv} corresponding to the SHL-vehicle using computed surface displacement. 8. Need for any mitigation strategy based on the determined FWD_{equiv}.

E^* = dynamic modulus; FOS = factor of safety; FWD_{equiv} = equivalent falling weight deflectometer load level.

Table 10. Inputs and outputs for module B3: Service limit.

Inputs	Outputs
1. Pavement structure. 2. Representative nucleus of SHL-vehicle configuration. 2.1. Axle spacing. 2.2. Tire spacing. 2.3. Tire pressure. 2.4. Tire loading. 3. SHL truck speed. 4. Field damage E^* master curve of existing AC-layer mixture. 5. Analysis temperature. 6. Material properties under SHL truck. 6.1. M_R of base layer. 6.2. M_R of SG layer. 7. Estimated SG τ_{max} parameters.	1. Investigation of the failure development in the sloped shoulder. 2. Need for any mitigation strategy based on slope stability analysis.

E^* = dynamic modulus.

Table 11. Inputs and outputs for module B4: Buried utility.

Inputs	Outputs
1. Pavement structure. 2. Representative nucleus of SHL-vehicle configuration. 2.1. Axle spacing. 2.2. Tire spacing. 2.3. Tire pressure. 2.4. Tire loading. 3. SHL truck speed. 4. Field damage E^* master curve of existing AC-layer mixture. 5. Analysis temperature. 6. Material properties under SHL truck. 6.1. M_R of base layer. 6.2. M_R of SG layer.	1. FOS against circumferential stress failure. 2. Check for pipe ovality. 3. Check for ring buckling stress. 4. Check for wall crushing stress. 5. Need for any mitigation strategy based on buried utility analysis.

E^* = dynamic modulus; FOS = factor of safety.

Table 12. Inputs and outputs for module B5: Cost allocation.

Inputs	Outputs
1. Pavement structure. 2. Standard truck axle configuration. 2.1. Axle spacing. 2.2. Tire spacing. 2.3. Tire pressure. 2.4. Tire loading. 3. Standard truck speed. 4. Representative nucleus of SHL-vehicle configuration. 4.1. Axle spacing. 4.2. Tire spacing. 4.3. Tire pressure. 4.4. Tire loading. 5. SHL truck speed. 6. Field damage E^* master curve of existing AC-layer mixture. 7. Analysis temperature. 8. Material properties under standard truck. 8.1. M_R of base layer. 8.2. M_R of SG layer. 9. Material properties under SHL truck. 9.1. M_R of base layer. 9.2. M_R of SG layer. 10. Allowable AC distress before rehabilitation at desired reliability. 10.1. Allowable AC permanent deformation. 10.2. Allowable AC bottom–up fatigue cracking. 11. AADTT for pavement section. 12. Discount rate for present value calculation. 13. Maintenance/rehabilitation activity repair cost. 14. Performance models' local calibration factors. 14.1. AC permanent deformation: K_{r1}, K_{r2}, K_{r3}, B_{r1}, B_{r2}, B_{r3}. 14.2. AC bottom–up fatigue cracking: K_{f1}, K_{f2}, K_{f3}, B_{f1}, B_{f2}, B_{f3}. 14.3. Base permanent deformation: B1. 14.4. SG permanent deformation: B1. 15. Estimation of the number of standard trucks prior to the pass of the SHL truck pass. 16. Estimation of E^* value at the specific pavement temperature and SHL truck operational speed.	1. Cost associated with the AC permanent deformation. 2. Cost associated with the AC bottom–up fatigue cracking. 3. Cost associated with the base permanent deformation. 4. Cost associated with the SG permanent deformation.

M_R = resilient modulus; E^* = dynamic modulus; K_{r1}, K_{r2}, K_{r3}, B_{r1}, B_{r2}, B_{r3}, K_{f1}, K_{f2}, K_{f3}, B_{f1}, B_{f2}, *and* B_{f3} = calibration factors

3.3.1. Module B5: Cost Allocation

Figure 29 illustrates the developed GUI for module B5. In this GUI, the user first provides general inputs in the "General Inputs" panel and then selects the layer of interest. For AC layers, cost allocation analysis can be conducted for permanent deformation (rutting) and bottom–up fatigue cracking. For unbound layers, cost analysis can be conducted for permanent deformation (rutting) only. In all three cases, the user must enter the appropriate performance model

parameters. In figure 29, a sample cost allocation analysis for the AC layer is presented based on permanent deformation. The performance-model parameters for the analysis of interests should be entered in the "Distress Analysis Layer Selection" panel. A maximum number of five cost allocation analyses can be performed by SuperPACK. For a selected layer, the user must enter the appropriate performance models. Cost allocation is conducted by clicking "Run" in the same panel. The results are shown in two panels: "Summary of Results" and "View Results." In the "Summary of Results" panel, a table summarizes information regarding layer number, layer analysis (rutting or fatigue cracking), PDAC, and relative-damage factor. The "View Results" panel displays the damage curve (i.e., fatigue-cracking percentage or permanent deformation as a function of number of vehicle passes) for the selected analysis.

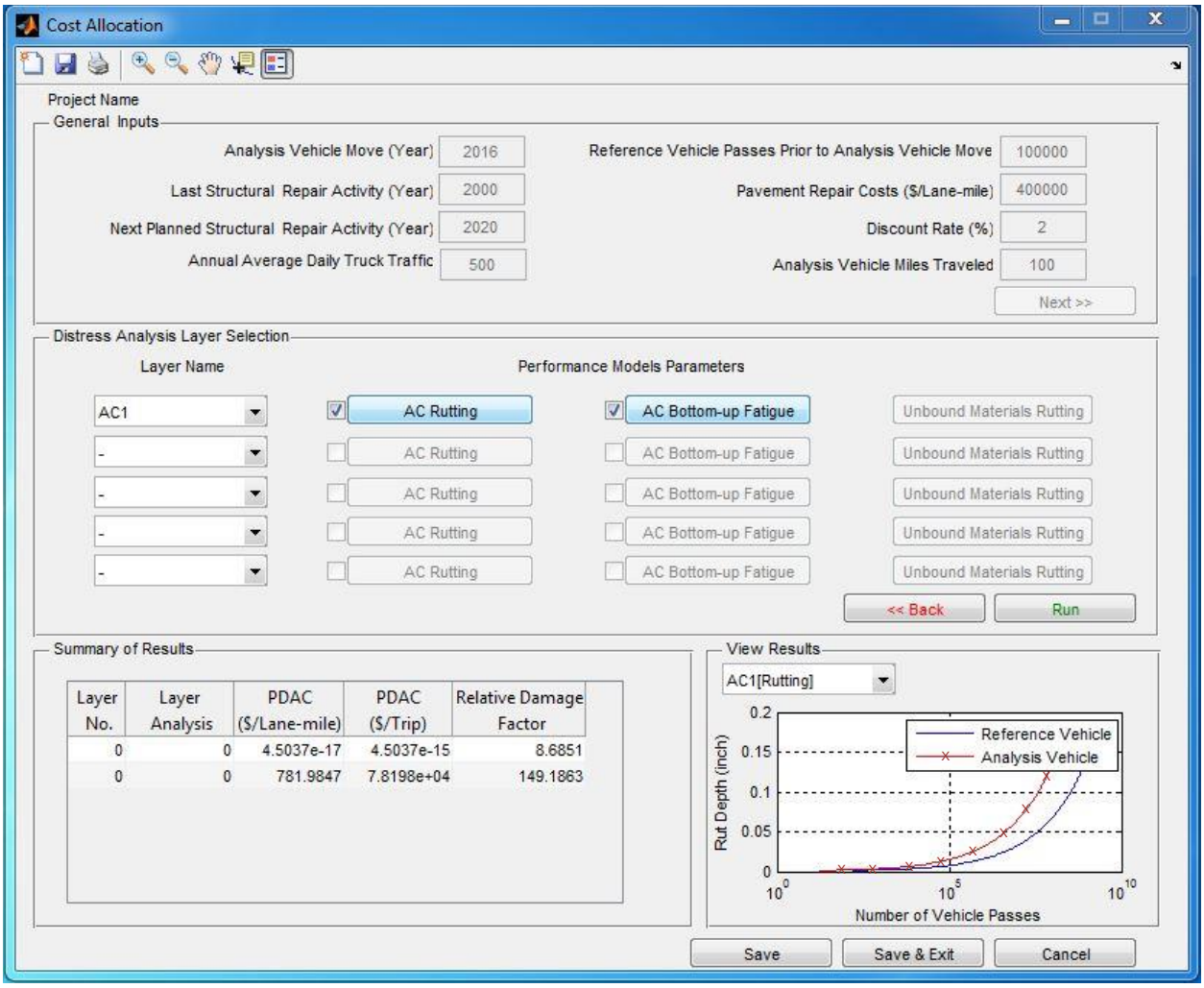

Figure 29. Screenshot. Module B5: Cost allocation.

3.4. SUMMARY

This chapter has presented the five A and five B modules implemented in SuperPACK and highlighted a few examples. The inputs needed for these modules, as well as the outputs they provide, are presented in table 3 through table 12.

Completing the A modules is a prerequisite for moving on to the B modules. Depending on the SHL-vehicle movement case being analyzed, the user has the option of executing some or all of the B modules. Screenshots of the SuperPACK GUIs for different modules were included to exemplify the use of those modules. The procedure to input required information in each module's GUI was explained through an example for each of the modules. A description on how to visualize each module output was also presented.

CHAPTER 4. SUMMARY, CONCLUSIONS, AND RECOMMENDATIONS

This volume addresses SuperPACK, which was developed in MATLAB as a stand-alone software package.[14] SuperPACK comprises three components: A modules, B modules, and an analysis engine. The analysis engine, 3D-Move ENHANCED, is based on the original formulation of 3D-Move.[10,12] However, several enhancements to the original formulation were incorporated in the SHL-vehicle movement analysis. For instance, runtime was improved using inverse Fourier transform, and parallel processing techniques were implemented so that different axle groups of an SHL vehicle could be analyzed in a reasonable amount of time.

The SuperPACK main window contains general information about the project, as well as basic information needed for a 3D-Move ENHANCED analysis (e.g., layer thicknesses, material types). The A and B modules can be accessed through the SuperPACK main window. A function and GUI were specifically developed for each module. Each GUI collects specific information needed to execute its corresponding module. Additionally, 3D-Move ENHANCED provides the modules with the necessary pavement responses when requested. The A and B modules share information through the SuperPACK main window.

A number of improvements could be incorporated into SuperPACK in future development. For instance, a Web-based version of the software can be developed so that authorities in highway agencies and engineers dealing with SHL movement can use SuperPACK online and share the information within their agency. Such an online platform can enhance coordination within an agency.

The current version of SuperPACK uses constant tire pressure with a circular tire–pavement contact area. However, 3D-Move ENHANCED is capable of handling nonuniform contact pressure that can be of any shape (not necessarily circular). Additionally, a database of SHL-vehicle tire pressures can be incorporated into SuperPACK. As of now, SuperPACK, along with 3D-Move ENHANCED, is capable of evaluating an SHL vehicle traveling at a constant speed, considering viscoelastic material characterization. Although viscoelastic material characterization is considered a significant advancement compared to classical multilayer linear elastic analysis, it can be improved by considering the effect of time variation of load (i.e., dynamic load) on pavement responses.[10]

The 3D-Move ENHANCED formulation allows for modeling tire shear stresses, such as forces due to SHL-vehicle braking and/or forces exerted on the pavement surface, while the SHL vehicle is travelling on a sloping pavement (i.e., uphill or downhill). Another potential improvement is the incorporation of backcalculation into the SuperPACK software. Currently, FWD backcalculation is conducted by the user externally in separate software, and results are entered into SuperPACK. The backcalculation procedure can be added directly into SuperPACK as a future enhancement option, eliminating the need for conducting backcalculation separately.

REFERENCES

1. Hajj, E.Y., Siddharthan, R.V., Nabizadeh, H., Elfass, S., Nimeri, M., Kazemi, S.F., Batioja-Alvarez, D.D., and Piratheepan, M. (2018). *Analysis Procedures for Evaluating Superheavy Load Movement on Flexible Pavements, Volume I: Final Report*, Report No. FHWA-HRT-18-049, Federal Highway Administration, Washington, DC.

2. Nimeri, M., Nabizadeh, H., Hajj, E.Y., Siddharthan, R.V., Elfass, S., and Piratheepan, M. (2018). *Analysis Procedures for Evaluating Superheavy Load Movement on Flexible Pavements, Volume II: Appendix A, Experimental Program*, Report No. FHWA-HRT-18-050, Federal Highway Administration, Washington, DC.

3. Nimeri, M., Nabizadeh, H., Hajj, E.Y., Siddharthan, R.V., and Elfass, S. (2018). *Analysis Procedures for Evaluating Superheavy Load Movement on Flexible Pavements, Volume III: Appendix B, Superheavy Load Configurations and Nucleus of Analysis Vehicle*, Report No. FHWA-HRT-18-051, Federal Highway Administration, Washington, DC.

4. Nabizadeh, H., Hajj, E.Y., Siddharthan, R.V., and Elfass, S. (2018). *Analysis Procedures for Evaluating Superheavy Load Movement on Flexible Pavements, Volume IV: Appendix C, Material Characterization for Superheavy Load Movement Analysis*, Report No. FHWA-HRT-18-052, Federal Highway Administration, Washington, DC.

5. Nabizadeh, H., Hajj, E.Y., Siddharthan, R.V., Nimeri, M., Elfass, S., and Piratheepan, M. (2018). *Analysis Procedures for Evaluating Superheavy Load Movement on Flexible Pavements, Volume V: Appendix D, Estimation of Subgrade Shear Strength Parameters Using Falling Weigh Deflectometer*, FHWA-HRT-18-053, Federal Highway Administration, Washington, DC.

6. Nabizadeh, H., Nimeri, M., Hajj, E.Y., Siddharthan, R.V., Elfass, S., and Piratheepan, M. (2018). *Analysis Procedures for Evaluating Superheavy Load Movement on Flexible Pavements, Volume VI: Appendix E, Ultimate and Service Limit Analyses*, Report No. FHWA-HRT-18-054, Federal Highway Administration, Washington, DC.

7. Nabizadeh, H., Siddharthan, R.V., Elfass, S., and Hajj, E.Y. (2018). *Analysis Procedures for Evaluating Superheavy Load Movement on Flexible Pavements, Volume VII: Appendix F, Failure Analysis of Sloped Pavement Shoulders*, Report No. FHWA-HRT-18-055, Federal Highway Administration, Washington, DC.

8. Nabizadeh, H., Elfass, S., Hajj, E.Y., Siddharthan, R.V., Nimeri, M., and Piratheepan, M. (2018). *Analysis Procedures for Evaluating Superheavy Load Movement on Flexible Pavements, Volume VIII: Appendix G, Risk Analysis of Buried Utilities Under Superheavy Load Vehicle Movements*, Report No. FHWA-HRT-18-056, Federal Highway Administration, Washington, DC.

9. Batioja-Alvarez, D.D., Hajj, E.Y., and Siddharthan, R.V. (2018). *Analysis Procedures for Evaluating Superheavy Load Movement on Flexible Pavements, Volume IX: Appendix H, Analysis of Cost Allocation Associated with Pavement Damage Under a Superheavy Load*

Vehicle Movement, Report No. FHWA-HRT-18-057, Federal Highway Administration, Washington, DC.

10. Seyed-Farzan, K. (2018). *3D-FAST: Three-Dimensional Fourier Analysis of Pavement Structures Under Transient Loading*, Dissertation, Department of Civil and Environmental Engineering, University of Nevada, Reno, NV.

11. Siddharthan, R.V., Yao, J., and Sebaaly, P.E. (1998). "Pavement Strain From Moving Dynamic 3D Load Distribution." *Journal of Transportation Engineering*, *124*(6), pp. 557–566, American Society of Civil Engineers, Reston, VA.

12. 3D-Move Analysis software v2.1. (2013). Developed by University of Nevada, Reno, NV. Available online: http://www.arc.unr.edu/Software.html#3DMove, last accessed September 19, 2017.

13. Kazemi, S.F. and Shafahi, Y. (2013). "An Integrated Model of Parallel Processing and PSO Algorithm For Solving Optimum Highway Alignment Problem." *Proceedings 27th European Conference on Modeling and Simulation*, pp. 551–557, ECMS, Alesund, Norway.

14. MATLAB. (2018). "MATLAB." (website) MathWorks, Natick, MA. Available online: https://www.mathworks.com/products/matlab.html?s_tid=hp_products_matlab, last accessed December 1, 2018.

15. National Cooperative Highway Research Program. (2004). *Guide for Mechanistic–Empirical Design of New and Rehabilitated Pavement Structures*, Transportation Research Board, Washington, DC.

16. Kenis, W.J. (1978). *Predictive Design Procedures, VESYS User's Manual: An Interim Design Method for Flexible Pavements Using the VESYS Structural Subsystem*, Report No. FHWA-RD-77-154, Pavement System Group, Structures and Applied Mechanics Division, Federal Highway Administration, Washington, DC.

17. DeJong, D.L., Pentz, M.G.F., and Korswagen, A.R. (1973). *Computer Program BISAR*, Koninklijke/Shell-Laboratorium, Amsterdam, Netherlands.

18. Huang, Y.H. (2004). *Pavement Analysis and Design*, Pearson Education, Cranbury, NJ.

19. Maina, J.W., De Beer, M., and Matsui, K. (2007). "Effects of Layer Interface Slip on the Response and Performance of Elastic Multi-Layered Flexible Airport Pavement Systems." International Conference on Maintenance and Rehabilitation of Pavements and Technological Control (MAIREPAV5), *Fifth Proceedings*, pp. 145–150, University of Iowa, Iowa City, IA.

HRDI-20/03-19(WEB)E